A 3-D model analysis of the slowdown and interannual variability in the methane growth rate from 1988 to 1997

James S. Wang,[1] Jennifer A. Logan,[1] Michael B. McElroy,[1] Bryan N. Duncan,[2] Inna A. Megretskaia,[1] and Robert M. Yantosca[1]

[1]Department of Earth and Planetary Sciences and Division of Engineering and Applied Sciences, Harvard University, 29 Oxford Street, Cambridge, MA 02138
[2]Goddard Earth Sciences and Technology Center, University of Maryland at Baltimore County, NASA Goddard Space Flight Center, Greenbelt, MD

Abstract. Methane has exhibited significant interannual variability with a slowdown in its growth rate beginning in the 1980s. We use a 3-D chemical transport model accounting for interannually varying emissions, transport, and sinks to analyze trends in CH_4 from 1988 to 1997. Variations in CH_4 sources were based on meteorological and country-level socioeconomic data. An inverse method was used to optimize the strengths of sources and sinks for a base year, 1994. We present a best-guess budget along with sensitivity tests. The analysis suggests that the sum of emissions from animals, fossil fuels, landfills, and waste water estimated using the IPCC default methodology is too high. Recent bottom-up estimates of the source from rice paddies appear to be too low. Previous top-down estimates of emissions from wetlands may be a factor of two higher than bottom-up estimates because of possible overestimates of OH. The model captures the general decrease in the CH_4 growth rate observed from 1988 to 1997 and the anomalously low growth rates during 1992-1993. The slowdown in the growth rate is attributed to a combination of slower growth of sources and increases in OH. The economic downturn in the former Soviet Union and Eastern Europe made a significant contribution to the decrease in the growth rate of emissions. The 1992-1993 anomaly can be explained by fluctuations in wetland emissions and OH after the eruption of Mt. Pinatubo. The results suggest that the recent slowdown of CH_4 may be temporary.

1. Introduction

Methane (CH_4) plays a major role in atmospheric chemistry and is the second most important anthropogenic greenhouse gas after carbon dioxide [Cicerone and Oremland, 1988; Ramaswamy et al., 2001]. CH_4 has an important influence on the oxidative capacity of the atmosphere, affecting both production and loss of the hydroxyl radical (OH), depending on the concentration of nitrogen oxides (NO_x). Oxidation of CH_4 can lead to formation of tropospheric ozone (O_3), an irritant that is harmful to the health of human beings and other living species and that acts also as a greenhouse gas. In the stratosphere, CH_4 moderates depletion of ozone, converting Cl_x (Cl + ClO) to the less reactive form HCl. Oxidation of CH_4 also increases the concentration of stratospheric H_2O, with chemical and radiative effects.

The mixing ratio of CH_4 has more than doubled over the past three centuries, from a pre-industrial average of about 700 parts per billion (ppb) to the present-day value of 1750 ppb [Etheridge et al., 1998; Blunier et al., 1993, Dlugokencky et al., 1998]. The growth rate began to slow in the 1980s [Steele et al., 1992], decreasing from about 14 ppbv/year (0.9%/year) in 1984 to close to zero during 1999-2000 [Dlugokencky et al., 1998; Simpson et al., 2002]. Superimposed on the long-term growth trend are large interannual fluctuations. The major sources and sinks of CH_4 have been identified (see Table 1), but their individual strengths and the causes of the observed concentration trends are not well known.

There is an ongoing debate as to the cause of the slowdown in the CH_4 growth rate and potential implications for future changes in CH_4. Dlugokencky et al. [1998] and Francey et al. [1999] suggested that the slowdown in the growth rate reflects a stabilization of CH_4, given that the observations are consistent with constant emissions and sinks since 1982. Another study suggested that a decrease in CH_4 over the next 50 years is a reasonable possibility given the recent slowdown in the growth rate and the existence of techniques and economic incentives to reduce emissions [Hansen et al., 2000]. However, others have argued that future concentrations of CH_4 are unpredictable given recent decoupling of human population growth and emissions, and uncertainties associated with the effects of global change on natural sources [Khalil and Rasmussen, 1993; Simpson et al., 2002]. Also, the recent slowdown in the growth rate may reflect the influence of an increasing sink rather than constant sources and sinks [Krol et al., 1998; Karlsdottir and Isaksen, 2000; Dentener et al., 2003]. An objective of the current study is to improve understanding of recent CH_4 trends in order to develop more reliable scenarios for future growth of CH_4 and hence its role in climate change and tropospheric and stratospheric ozone chemistry.

A variety of approaches have been used to estimate the contributions of individual sources and sinks to the overall budget of CH_4. These can be divided into "bottom-up" and "top-down" approaches. Bottom-up estimates rely on measurements at specific sites (e.g. for wetlands) or from specific sources (e.g. cattle) to determine emissions per unit area or per unit activity (referred to as "emission factors") under various conditions, extrapolated then to calculate regional and global totals using estimates of areal extent or activity data. Estimates from a number of bottom-up studies are included in Table 1 (the values in the "A Priori" column and the estimates by the U.S. EPA [2001; 2002]). Top-down estimates use measurements of CH_4 concentrations (and sometimes isotopic composition) representative of large spatial scales in combination with a chemical transport model (CTM) to infer strengths of sources and sinks. Results from such studies are included in Table 1 [Fung et al., 1991; Hein et al., 1997; Houweling et al., 1999]; the last two used formal inverse algorithms. These three studies computed long-term (several year) mean budgets for CH_4. There is notable scatter in the

estimates from the different studies summarized in Table 1, implying significant uncertainties in the budget.

Reaction with OH constitutes the main sink for CH_4. Bottom-up estimates for OH abundances involve estimates or simulations of distributions of OH precursor species and photochemical calculations to determine OH [e.g. Spivakovsky et al., 2000; Karlsdottir and Isaksen, 2000; Dentener et al., 2003]. Top-down methods for estimating OH rely on measurements of reactive trace gases, especially methyl chloroform (CH_3CCl_3), for which emissions are associated exclusively with industrial activity [e.g. Spivakovsky et al., 2000; Prinn et al., 2001; Krol and Lelieveld, 2003].

Studies seeking to explain the slowdown in CH_4 growth rate over the past two decades have focused on one or a few of the individual source or sink processes. Khalil and Shearer [1993], for example, noted that the global cattle population and the area devoted to rice paddies had leveled off in the 1980s relative to previous decades, and that these trends may have contributed to the slowdown. Others have proposed that changes in rice irrigation and fertilization practices may have resulted in reductions in emissions from rice paddies [e.g. Li et al., 2002; Denier van der Gon, 1999]. A number of studies have suggested that wet deposition of sulfate in wetlands and rice paddies could have suppressed bacterial production of CH_4 [e.g. Gauci et al., 2002; van Bodegom et al., 2001]. Stevens [1988], based on the positive trend in the $\delta^{13}C$ (ratio of ^{13}C to ^{12}C) of CH_4 observed at a number of sites around the world, suggested that natural sources depleted in ^{13}C such as wetlands and CH_4 hydrates might have decreased. The EDGAR inventory (Version 3.2) [Olivier, 2002] and an analysis by E. Matthews [personal communication] represent previous efforts to estimate interannually varying emissions from a large number of sources using a bottom-up approach. Both studies found that the growth rate of global anthropogenic CH_4 emissions had decreased significantly since the late 1980s. Karlsdottir and Isaksen [2000] reported results from a 3-D CTM simulation of OH, accounting for interannually varying NO_x, carbon monoxide (CO), CH_4, and non-methane hydrocarbons (NMHC), but not for variations in column ozone. They obtained a positive trend for OH of 0.43%/yr from 1980 to 1996, and demonstrated through mass balance that the trend in OH allows for a positive trend in CH_4 emissions, rather than for the constant emissions deduced by some studies. Bekki et al. [1994] examined the impact of changes in the ozone column on OH production and found that they could explain part of the change in CH_4 growth over the first half of the 1980s.

Other studies have tackled specific aspects of the CH_4 cycle seeking to explain anomalies in growth rates observed from 1991 to 1993. The growth rate was high in the latter part of 1991 and low during 1992-1993 [Dlugokencky et al., 1994a; Dlugokencky et al., 1998]. Many of the proposed explanations invoke effects of the eruption of Mt. Pinatubo in the Philippines in June 1991. Dlugokencky et al. [1996] used a radiative transfer model to demonstrate that the high abundance of absorbing SO_2 and scattering sulfate aerosols in the stratosphere originating from the eruption significantly decreased production of OH in the troposphere for the latter part of 1991, resulting in higher rates of accumulation of CH_4. Bekki et al. [1994] found that the increase in OH that they modeled for 1992, caused by stratospheric ozone depletion promoted by long-lived aerosols from the eruption, could account for half the observed drop in the growth rate of CH_4 that year. A possible increase in the rate of stratosphere-troposphere exchange due to aerosol heating of the lower stratosphere was considered by Schauffler and Daniel [1994] in a box model. They concluded that this could have contributed to the decrease in growth rate observed for CH_4 as well as for N_2O and CO_2. Hogan and Harriss [1994], Bekki and Law

[1997], and Walter et al. [2001a,b] proposed that lower temperatures and lower precipitation in the aftermath of the Pinatubo eruption could have suppressed emissions from wetlands. Explanations for the anomalous decrease in the growth rate that do not involve Mt. Pinatubo include decreases in natural gas leakage in the former Soviet Union resulting from decreases in production during the transition to a market economy and improved maintenance of formerly leaky pipelines [Dlugokencky et al., 1994a,b; Law and Nisbet, 1996; Lowe et al., 1994], and decreases in biomass burning in Southern Africa due to low fuel loads induced by drought and in the Amazon due to unusual climatic conditions [Lowe et al., 1994; 1997]. The studies by Lowe et al. relied on measurements of $\delta^{13}C$ as well as concentrations of CH_4 to form their conclusion. Gupta et al. [1996], however, argued that a variety of source/sink change combinations could be consistent with the observed changes in CH_4 concentration and isotopic composition. Furthermore, different measurement programs have produced conflicting trends in $\delta^{13}C$ for the period 1991-1993 [Etheridge et al., 1998; Quay et al., 1999].

In this study, we use a combination of top-down and bottom-up approaches to quantify the interannually varying budget of CH_4 for the period 1988-1997. We utilize the 3-D GEOS-CHEM CTM [Bey et al., 2001] with interannually varying emissions, meteorology, and chemical sinks. This study builds on a previous analysis of the budget of CO using the same model [Duncan et al., 2003b,c]. In that work, tropospheric OH and CO fields were calculated for 1988-1997 allowing for interannual variations in meteorology, column ozone, CH_4, and emissions of CO; CH_4 distributions were prescribed based on surface observations [Dlugokencky et al, 2001]. The current study uses the OH fields from the CO simulation. Interannual variations of CH_4 sources are based on socioeconomic, meteorological, and other data, and an inverse technique is employed to optimize absolute strengths of sources and sinks for a base year, selected as 1994. The sources and sinks are incorporated in the CTM, which is run in a forward manner from 1988 to 1997. Resulting distributions of CH_4 are evaluated using surface and aircraft observations.

Details of the model and methods are described in section 2. An evaluation of the interhemispheric mixing in the model is presented in section 3.1. Trends in anthropogenic sources of CH_4 for different geographic regions are discussed in 3.2. The budget for the base year derived from the inversion approach is presented in 3.3. Section 3.4 presents evaluations of the interannual simulations and our proposed explanations for the slowdown and interannual fluctuations in the growth rate of CH_4. Future trends in the factors influencing CH_4 are discussed in section 4. Conclusions are presented in section 5.

2. Model and Methods

2.1. GEOS-CHEM CTM

We used the GEOS-CHEM 3-D global CTM [Bey et al., 2001], driven by assimilated meteorological observations from the Goddard Earth Observing System (GEOS) of the NASA Global Modeling and Assimilation Office (GMAO, formerly Data Assimilation Office (DAO)). The work shown here employed version 5.02 of GEOS-CHEM for transport (http://www-as.harvard.edu/chemistry/trop/geos/geos_versions.html). Meteorological fields, updated every 3 or 6 hours, include winds, surface pressures, temperatures, specific humidities, wet convective mass fluxes and detrainment rates, column cloud fractions, cloud optical depths, precipitation, surface albedos, roughness heights, friction velocities, and mixing depths. The CTM was run with a resolution of 4° latitude by 5° longitude. The CTM has either 20 or 26 sigma layers in the vertical, depending on the parent GCM version: for January 1988-November 1995, the version is GEOS-1 with 20 layers, spanning the altitude range 0 to 31 km, or up to 10 hPa (12 layers are

located below 250 hPa or ~10 km), and for December 1995-December 1997, the version is GEOS-STRAT with 46 layers (0 to 65 km (0.1 hPa)), the upper 23 of which are combined into 3 layers in the CTM (14 layers are below 250 hPa). Since the meteorology in our multi-year simulations was derived from two different versions of the assimilation model, we were concerned that the results could be influenced by a spurious change in meteorological parameters between November and December of 1995. For example, the trend in the OH radical could be affected by a change in cloudiness, precursor transport, etc. From a comparison of meteorological fields between the two GCM versions, we concluded that differences appear to be small.

Conservation of tracer mass in a CTM is critical for studies of the CH_4 budget, given the long lifetime of the gas, ~10 years [Prather et al., 1987; Jöckel et al., 2001]. The data assimilation system for the parent GCM of our CTM is not constrained to conserve dry air mass [S.-J. Lin, personal communication]. As a consequence, tracer mass in the CTM would not be conserved if the surface air pressures calculated after each advection step in the CTM were replaced with the archived GCM surface pressures, a typical procedure when CTMs are run "offline". We chose therefore to run the CTM in "floating pressure mode," for which CTM-calculated pressures are retained rather than replaced by GCM pressures [P. Cameron-Smith, personal communication; Rotman et al., 2003]. This ensures that mass is conserved. In order that CTM pressures not deviate significantly from those of the GCM, we incorporated the pressure-fixer developed by Prather et al. [1987], which adjusts horizontal mass fluxes between adjacent grid boxes before each advection time step to minimize the difference between CTM and GCM pressures.

Accurate simulation of interhemispheric mixing is important also for long-lived species [Prather et al., 1987; Jacob et al., 1987; Houweling et al., 1999]. We evaluated interhemispheric mixing in the model using simulations of ^{85}Kr, a long-lived species emitted in relatively well known amounts exclusively from the Northern Hemisphere during reprocessing of nuclear fuel and removed from the atmosphere solely by radioactive decay (e-folding lifetime = 15.52 years). In this we followed the methodology described by Jacob et al. [1987]. The interannually varying emissions from 1978 to 1983 were adopted from Von Hippel et al. [1986] and Jacob et al. [1987], and model results were evaluated using observations of ^{85}Kr from cruises in the Atlantic Ocean between 84°S and 52°N during 1980-1983 [Weiss et al., 1983; Von Hippel et al., 1986]. The model was spun up for two years using emissions of ^{85}Kr estimated for 1978-1979 with initial conditions based on the latitudinal profile of ^{85}Kr observed for 1980, scaled by a factor of 0.913 to adjust for the difference in global emissions between 1978 and 1980. Model results were compared with observations from 1980-1983. To evaluate the GEOS-1 meteorological parameters, the model was run using meteorology for 1988-1993, while for GEOS-STRAT, the meteorology was recycled for 1996-1997. Although the meteorology and emissions/observations are for different time periods, it is expected that effects of interannual variations in meteorology should be averaged out, given that the comparison of the model with observations covers several years.

2.2. Chemical Sinks of Methane

For this study, interannually varying monthly distributions of tropospheric OH were taken from the study of CO conducted by Duncan et al. [2003b]. In that work, OH was calculated for the period 1988-1997 using a parameterization developed by Duncan et al. [2000]. Use of the parameterization saves computational time, permitting a large number of multi-year

simulations. The concentration of OH for a given grid box is calculated as a function of a set of variables including temperature, latitude, declination, cloud albedo, overhead ozone column, the concentrations of ozone, water vapor, CO, nitrogen oxides, and hydrocarbons, and others. The GMAO fields were adopted to define the meteorological variables. Semi-hemispheric, annual mean concentrations of CH_4 from 1988 to 1997 were prescribed based on surface observations from the CMDL network [Dlugokencky et al., 1994b; 2001]. Tropospheric concentrations of O_3, NO_x, isoprene, acetone, and other species were taken from a full chemistry run of the GEOS-CHEM model for the period September 1996 to August 1997 [*Martin et al.,* 2002]. Interannual emissions of CO were prescribed, and OH and CO concentration fields were calculated interactively. Sources of interannual variability in OH include meteorology, overhead ozone columns, CO, and CH_4. Column abundances of ozone were taken from monthly observations by the Total Ozone Mapping Spectrometer/Solar Backscatter Ultraviolet instrument (TOMS/SBUV) [R. Stolarski, *personal communication*, 2001; http://code916.gsfc.nasa.gov/Data_services/merged/index.html].

Loss rates for CH_4 in the stratosphere were adapted from a stratospheric model [Schneider et al., 2000; D. Jones, personal communication]. Losses varied from month to month; interannual variability was not taken into account. The stratospheric sink accounts for 5-8% of total loss of CH_4 in our budget.

2.3. Emissions

The geographic and seasonal distributions of the CH_4 sources and the soil sink were based on Fung et al. [1991], except for emissions from biomass burning and biofuels, for which we used databases developed at Harvard [Duncan et al., 2003a; Yevich and Logan, 2003]. The distributions in Fung et al. for some of the sources were based in turn on studies by Matthews and Fung [1987] for wetlands, Matthews et al. [1991] for rice paddies, Lerner et al. [1988] for domesticated animals, and Matthews [1983] for vegetation type (used for the termite source and soil sink). We neglected a few of the minor sources, including oceans and freshwaters (~10 Tg/yr) [Fung et al., 1991], and volcanoes (~3.5 Tg/yr) [Lacroix, 1993]. We did not explicitly consider emissions from wild animals, fossil fuel combustion, and industrial processes, but since these are co-located with some of the larger sources that were considered, they are effectively incorporated in the results of the inversions described below. Source strengths in Fung et al. were estimated using country- and province/state-level socioeconomic data such as livestock populations, rice harvest area, and fossil fuel production, applying regional emission factors for each process. The emissions were distributed spatially using maps of human population densities, land use, coal mine and gas and oil well locations, wetlands, etc. Seasonal distributions for the rice and wetland sources were based on rice crop calendars and meteorology, respectively. In this study, interannually varying distributions were estimated by adjusting those of Fung et al. to account for yearly country-by-country socioeconomic and other data. Since their distributions were based largely on data for 1984, we multiplied the emissions in each of their grid cells by the ratio of the socioeconomic variable between the year of interest and 1984, on a country by country basis. For the source from domesticated animals, we considered the populations of cattle, water buffalo, and sheep only, these being the dominant emitters [Lerner et al., 1988], weighted by average emission per individual. Table 2 lists the socioeconomic and other variables used to model the interannual variability in the sources along with the sources of the data. The interannual variability was expected to be minor for termites, hydrates, landfills and waste water, and the soil sink. Our method for estimating the interannual

variability of sources assumed constant emission factors over the simulation period, and thus it did not account, for example, for changes in leakage rates from pipelines or efforts to recover and utilize CH_4 emitted from landfills and coal mines.

Following Fung et al. [1991], we considered three types of wetlands: swamps, which occur mainly at low to middle latitudes, bogs, which occur mainly at high latitudes of the Northern Hemisphere, and tundra, which occurs in the far north. We assumed that wetland emissions are controlled mainly by soil temperature and precipitation based on the results of a process-based wetland emission model [Walter et al., 2001a,b]. Lacking the full emissions fields from that study, we estimated monthly and interannual variations using historical data for soil temperature and precipitation, and calculating emissions anomalies for each month according to the temperature and precipitation sensitivities reported in Walter et al. [2001b]. In that study, a ±1° change in temperature was estimated to contribute a change of about ±20% in emissions for all ecosystems, while a ±20% change in precipitation was associated with a change in global emissions by about ±8%; the latter effect varied with latitude, ranging from a change in emissions of about ±4% in the tropics to about ±33% in boreal regions (Figure 3 in Walter et al. [2001b]). We used meteorological fields from the National Center for Environmental Prediction (NCEP) reanalyses for 1988-1997, thus avoiding possible inconsistencies caused by a change in the GMAO assimilation model version. The wetland emissions fields of Fung et al. were adopted as a baseline, to which we added the monthly emissions anomalies to establish interannual variations in emissions.

Interannually varying emissions of CH_4 from biomass burning rely on the work of Duncan et al. [2003a]. In brief, a mean inventory of the quantity of biomass burned was developed by J.A. Logan and R. Yevich as summarized by Lobert et al. [1999]. Emission factors for CH_4 for different vegetation types and regions were based on the recommendations of Andreae and Merlet [2001]. Temporal variability was imposed using TOMS Aerosol Index (AI) data. There is a gap in the AI data from May 1993 to July 1996, which Duncan et al. partly filled using burn area data for Canada and Alaska and literature estimates for forest fires in Indonesia.

2.4. Observations

Observations of CH_4 from a global network of surface air sampling sites operated by the National Oceanic and Atmospheric Administration (NOAA) Climate Monitoring and Diagnostics Laboratory (CMDL) [Dlugokencky et al., 1994b] were used for model evaluation. Sites containing at least several years of data in the study period are listed in Table 3. We calculated monthly means using the weekly samples, including non-background observations as long as they were duplicated. In comparing model results with the CMDL observations, an adjacent model grid box was sampled if the grid box corresponding to the site included significant emissions; this was necessary to more closely simulate the observations, since the CMDL sampling protocol involves when possible selection of clean wind sectors (e.g. offshore). Sites and the grid boxes sampled in this manner were Key Biscayne (1 box to east), Tae-ahn Peninsula (south), Cape Grim (southwest), Barrow (north), Cape Meares (west), Mace Head (west), and Baltic Sea (northwest).

Observations from aircraft campaigns were used to evaluate the vertical distributions of CH_4. These campaigns included ABLE-3A, over Alaska in July 1988, ABLE-3B, over Canada in July 1990, PEM-West A, over the Western Pacific in October 1991, TRACE-A, over the South Atlantic and adjacent continents in September 1992, PEM-West B, over the Western Pacific in February 1994, and PEM-Tropics A, over the Pacific in September 1996. Data were

binned and averaged by region and altitude for comparison with the same region in the model. The regions are shown in Wang et al. [1998].

2.5. Inversion Methods

We used a Bayesian inverse approach to determine the absolute strengths of the sources and sinks for CH_4. This approach uses observations of CH_4 to optimize source and sink strengths (= parameters), subject also to constraints provided by previous, or "a priori," estimates. Specifically, the difference between model and observed concentrations at a set of sites and the difference between a priori and a posteriori parameter estimates are minimized simultaneously in a least-squares manner [Rodgers, 2000]. Both the observations and the a priori estimates are weighted by estimates of uncertainties. The following defines the solution for the set of parameters:

$$\hat{\mathbf{x}} = \mathbf{x}_a + (\mathbf{K}^T \mathbf{S}_\varepsilon^{-1} \mathbf{K} + \mathbf{S}_a^{-1})^{-1} \mathbf{K}^T \mathbf{S}_\varepsilon^{-1} (\mathbf{y} - \mathbf{K}\mathbf{x}_a),$$

where
$\hat{\mathbf{x}}$ is the vector of a posteriori parameter estimates
$\mathbf{x}_a$ is the a priori parameter estimates
$\mathbf{K}$ is the Jacobian matrix
$\mathbf{S}_\varepsilon$ is the observation error covariance matrix
$\mathbf{S}_a$ is the a priori parameter error covariance matrix
$\mathbf{y}$ is the vector of observations.

The a posteriori parameter error covariance matrix is given by

$$\hat{\mathbf{S}} = (\mathbf{K}^T \mathbf{S}_\varepsilon^{-1} \mathbf{K} + \mathbf{S}_a^{-1})^{-1},$$

with the square roots of the diagonal elements providing estimates of a posteriori parameter uncertainties.

The inversion was implemented for 1994, a period for which many CMDL sites were in operation; sites with at least 8 months of data were used (see Table 3). The observed global total growth of CH_4 for 1994 was also used as a constraint on the parameter estimates [Dlugokencky et al., 2001]. Observations were weighted by the observation errors, estimated as the sum of transport error (0.5% of the observed mixing ratio) and representation error (i.e. the mismatch between the point measurements and the monthly mean over the grid box). Measurement precision (~0.2% [Dlugokencky et al., 1994b]) is a relatively small source of uncertainty and was excluded from the error analysis. Errors were assumed to be uncorrelated. We used the standard error of the monthly mean calculated from weekly samples as a proxy for the representation error. The estimate for the transport error was based on analysis of deviations of CO simulated using GEOS-CHEM from observations during the TRACE-P aircraft campaign in the northwest Pacific in 2001 [Palmer et al., 2003]. Those error estimates were extrapolated to the entire Northern Hemisphere using comparisons of pairs of chemical forecasts of CO [Jones et al., 2003]. The 10%-30% error determined therein for CO in cleaner regions was adjusted to 0.5% for CH_4 to account for the smaller relative variability in CH_4 concentrations and the use of monthly means in this study. To verify that the value assumed for transport error was appropriate, we tested several different magnitudes for the assumed transport error and found that the value of 0.5% produced a chi-squared (cost function) value for the a posteriori budget close to 1 (normalized), the expected value for a satisfactory retrieval [Marks and Rodgers, 1993]. In contrast, a transport error of 5% resulted in a chi-squared of 0.04, indicating that the retrieval fits the observations more tightly than expected and that the assumed observation errors should be decreased.

We inverted for the annual global strengths of individual source and sink types, fixing the spatial and seasonal distributions, in a manner similar to Hein et al. [1997]. Thus, possible inaccuracies in the distributions are a source of error that was not taken into account in our formal error analysis. Sources and sinks with similar spatial distributions (e.g. fossil fuels, landfills/waste water, animals, and soil oxidation) were aggregated as a single parameter for purposes of the inverse calculations, since the observations cannot distinguish between co-located sources. Table 4 lists the set of parameters included in the analysis. A priori values for the parameters and their uncertainties were based on bottom-up estimates where possible. The emission totals from the EDGAR 3.2 inventory for year 1995 were used for most of the anthropogenic sources, including enteric fermentation and waste from domesticated ruminants, landfills and waste water, gas venting/flaring, gas leakage, coal mining, and rice paddies [Olivier, 2002]. We used our own a priori estimates for the biomass burning and biofuel sources [Duncan et al., 2003a; Yevich and Logan, 2003]. The a priori estimate for wild ruminants (5 Tg) was taken from Lelieveld et al. [1998]; soil absorption from Ridgwell et al. [1999]; termites from Sanderson [1996]; hydrates from Fung et al. [1991]; wetlands from Walter et al. [2001a]; the tropospheric OH sink strength from a CH_4 simulation using the OH fields from Duncan et al. [2003b]; and the stratospheric sink strength from Hein et al. [1997].

We employed a technique of linearly decomposing the total CH_4 concentration into contributions from individual sources and sinks, similar in concept to the approach of Fung et al. [1991], to compute efficiently the total concentrations for different combinations of source and sink strengths. In a "tagged CH_4 tracer run", each source/sink type was simulated separately for year 1994 using the CTM, starting from zero concentration, emitting or destroying 1 Tg of CH_4 over the year, and accumulating parts per billion of CH_4 (negative concentrations in the case of sinks). The tagged tracer run also provided the elements for the Jacobian matrix (the sensitivities of monthly CH_4 concentrations at each site to a unit emission/loss from each source/sink). The distribution of total CH_4 was fixed in calculating losses due to reaction with tropospheric OH, i.e. the OH sink tracer was not run interactively with the sources and other sinks. This 3-D monthly varying CH_4 distribution, constrained to match observations for 1994 as closely as possible, was derived using the following procedure. First, a preliminary tagged tracer run was implemented in which zonal averages for CH_4 were specified based on CMDL observations to calculate the OH sink tracer. An inversion was then carried out using the results of this tagged tracer run. The a posteriori model concentrations provided the CH_4 distribution used in a refined OH sink tracer run.

To calculate the total CH_4 concentration, we needed to account for the effects of emissions and losses from all years prior to the year of interest. Thus, we ran also an "initial condition tracer" for 1994. In this, a CH_4 field, constrained to match CMDL observations at the beginning of the year through an inversion procedure for 1993, was advected and mixed with no emissions or losses. The contributions from individual sources/sinks during 1994, multiplied by the desired strengths, were added then to the initial condition tracer fields. We verified that the resulting CH_4 distribution is equivalent to that produced by a single model run in which all the sources and sinks are introduced interactively.

2.6. Interannual Simulation Methods

To initialize the multi-year simulations, we ran the CTM for 1987, using source and sink strengths determined on the basis of an inversion for that year. Concentrations from the end of that simulation were used as initial conditions for the multi-year simulations. The CTM was run

from 1988 through 1997, applying emissions determined from the 1994 inversion and extrapolated to the other years using the socioeconomic and other data, and applying sinks scaled to the 1994 inversion results. To apply the interannual scaling factors, the inversion result for the aggregate parameter comprising the animal, fossil fuels, and waste sources and the soil sink was disaggregated based on the a priori ratios among the individual sources/sink. At the November-December 1995 transition between model versions, the concentration fields were regridded in the vertical from 20 to 26 levels through interpolation and extrapolation.

In addition to comparing the model and CMDL raw time series, we calculated instantaneous growth rate time series for the model and observations, a procedure intended to highlight interannual variations. The method adopted to calculate the growth rate time series is similar to that described by Thoning et al. [1989]. A second-order polynomial and a set of four harmonics were used to fit the concentration time series for each site, using multiple linear regression. The residuals of the curve fit were smoothed, using a loess smoother with a span of 2 years to filter out short-term fluctuations. The smoothed residuals were added to the polynomial portion of the curve fit (in effect deseasonalizing the time series), and the derivative of the series was evaluated and smoothed with a span of 1 year to obtain the instantaneous growth rate. Our method leads to results for the observations similar to those reported by the CMDL [ftp://ftp.cmdl.noaa.gov/ccg/figures/ch4trend_mlo.ps; Dlugokencky et al., 1994a].

3. Results

3.1. Evaluation of Interhemispheric Mixing

The latitudinal distribution of ^{85}Kr in the Atlantic Basin (30°W) computed using GEOS-1 and GEOS-STRAT meteorological parameters is compared with observations in Figure 1. Both versions of the model reproduce the magnitude of the observed latitudinal gradient for each of the cruises, including the large jump near 0° marking the barrier to interhemispheric mixing at the intertropical convergence zone. Another measure of the accuracy of the model's mixing is the interhemispheric exchange time, defined as the difference between the mean concentrations in the Southern and Northern Hemispheres, divided by the net cross-equatorial flux of tracer [Prather et al., 1987]. We calculated an exchange time of 1.0 year for GEOS-1 and 1.1 years for GEOS-STRAT, close to the value of 1.1 years determined by Jacob et al. [1987]. This contrasts with results from a number of previous CH_4 studies, in which the interhemispheric mixing was too slow (e.g. Hein et al., 1997; Houweling et al., 1999). Hein et al. report that their CTM overestimated the interhemispheric gradient of CH_3CCl_3 by 12%, and that an earlier simulation of CFC-11 had revealed an overestimate of the interhemispheric exchange time of ~20%; Houweling et al. used the same CTM. Those authors conceded that the inaccurate treatment of interhemispheric mixing had a significant effect on budgets calculated for CH_4.

3.2. Trends of Sources

Time series of emissions from different anthropogenic sources by region, calculated using the socioeconomic data, are displayed in Figure 2a-d. The figures illustrate the steady increase in emissions from natural gas consumption and production over the analysis period for much of the world outside of Eastern Europe and the former Soviet Union (FSU). Globally, emissions from gas leakage increased by 14% from 1988 to 1997. There were increases also in emissions from domesticated animals and coal mining for many developing countries. The trends indicated here suggest that there is potential for significant further growth in CH_4 emissions in the future.

A key feature in Figure 2 is the dramatic decrease in all anthropogenic sources for Eastern Europe and the FSU over the analysis period. Emissions decreased by 4.0 Tg, or 38%, for the ruminant source between 1989 and 1997; by 2.6 Tg, or 18%, for the gas leakage source; by 2.4 Tg, or 42%, for the coal mining source; and by 10.0 Tg, or 25%, for the total anthropogenic source. The drop in emissions from animals is driven by sharp declines in livestock populations; in the case of cattle, the dominant emitter, the decrease was ~50% in the FSU, and for the sum of Eastern Europe and the FSU, the decrease corresponded to close to 5% of the global population. Production of natural gas in the FSU, one of the world's most important natural gas producing regions, dropped by 18% from 1990 (the peak year) to 1997 [http://www.eia.doe.gov/emeu/international/gas.html]. The decreases in the CH_4 sources are associated with the transition from a centrally-planned to a market economy in the early 1990s and the ensuing recession. For example, large cattle populations and high consumption of beef in Russia were bolstered in earlier years by government subsidies, which were removed during the economic transition [Sedik, 1993].

Our calculations indicate that the economic downturn in Eastern Europe and the FSU had a significant impact on the global trend of CH_4 emissions over the 1990s, in agreement with recent assessments by the U.S. Environmental Protection Agency (EPA) [EPA, 2001] and Olivier [2002]. Without the decline in emissions from that region, global emissions from anthropogenic sources would have grown at a faster rate than over the past decade and there would have been less of a decline in the growth rate of atmospheric CH_4.

3.3. Base Year Budget

We present results from three different inversions, in which: 1) the tropospheric OH sink strength was included as a parameter to be determined by the inversion, 2) the tropospheric OH sink strength was fixed at its a priori value (calculated using the parameterized OH), and 3) the tropospheric OH sink strength was fixed at a value derived from an inversion using observations of methyl chloroform (abbreviated MCF here). Results from the third case are considered to represent our best guess for the budget. The first case yielded the surprising result that the a posteriori strength of the OH sink was much lower—by 38%--than the a priori value, outside the assigned 2σ uncertainty range. The equivalent tropospheric average OH concentration would be 10% lower than an estimate reported previously by Prinn et al. [2001] and 27% lower than that of Spivakovsky et al. [2000]; the resulting lifetime for MCF with respect to tropospheric OH is outside the 2σ uncertainty range of the estimate quoted by Prinn et al. [2001] based on analysis of MCF observations. To understand this discrepancy, we conducted our own MCF inversions, taking advantage of the simpler budget of the gas and the relatively well known spatial distribution of emissions. These calculations confirm that the a priori value for OH is too high, although the decrease in OH relative to previous studies is not as extreme, e.g. ~10% below the estimate of Spivakovsky et al. [2000]. A major difference between our method and those of previous MCF inversion studies [Prinn et al., 2001; Krol and Lelieveld, 2003] is that we optimized MCF emissions as well as the OH sink. The results indicate that the emissions assumed by previous studies for the 1980s (prior to the ban on the production of MCF in developed countries), based on the work of Midgley and McCulloch [1995], may be too high, by about 10%. Assuming the MCF sales data in Midgley and McCulloch are accurate, the above result suggests that the time lag between sales and emissions may have been underestimated. The idea of a longer delay was proposed also by Krol et al. [2003] and Barnes et al. [2003]. Another improvement over previous studies is that we use a transport model with meteorology

specific to the period of the study and with higher spatial resolution. Krol and Lelieveld [2003] demonstrated that inversions for OH are sensitive to the treatment of transport. There is evidence also from recent photochemical model calculations of tropospheric OH that previous estimates for OH may be too high. Full-chemistry simulations for 2001 with the GEOS-CHEM model that account for recent improvements in reaction rate coefficients and chemical mechanisms indicate a lifetime for MCF with respect to tropospheric OH of 6.4-6.8 years [A. Fiore, R. Park, personal communication], longer than the lifetime of 5.99 ± 1.66 years computed by Prinn et al. [2001] and the value of 5.7 years computed by Spivakovsky et al. [2000]. The improvements in the model include an upward revision of the rate coefficient for the $O(^1D) + N_2$ reaction based on the work of Ravishankara et al. [2002], which results in a reduction in the rate for production of OH. The results of our MCF study indicate that current understanding of MCF emissions, global OH concentrations, and lifetimes of reactive trace gases may be subject to significant revision. The work on MCF will be presented in detail elsewhere.

The second CH_4 inversion (OH fixed at the a priori value) is included in the discussion in the rest of the paper to illustrate the sensitivity of the inversion results for CH_4 sources as well as to demonstrate that the main conclusions regarding the interannual variability of CH_4 are independent of the budget assumed for the base year. We refer to the first inversion as "Low OH", the second as "High OH", and the third as "Best Guess".

The inversion results are compiled in Table 4. We verified that the a posteriori budgets are consistent with isotopic constraints. Model values for the average $\delta^{13}C$, δD, and fossil fraction of the source are compared in Table 4 with estimates based on atmospheric measurements of CH_4 isotopic composition by Quay et al. [1999]. The values for all three inversions lie within the uncertainty range quoted by Quay et al. Also shown in Table 4 are the lifetimes of CH_4 and MCF with respect to tropospheric OH and the tropospheric mean OH concentration for the three inversions along with corresponding estimates from the literature. The lifetime of CH_4 with respect to OH for the "Low OH" case is 43% longer than the estimate by Prinn et al. [2001] and outside the uncertainty range. The lifetime for the "High OH" case is 10% shorter than the estimate by Prinn et al. but within the uncertainty range. The lifetime for the "Best Guess", 11.3 years, is 12% longer than the Prinn et al. value but within the uncertainty range. The "Best Guess" lifetime is 18% longer than the value of 9.6 years adopted by the Third Assessment Report of the Intergovernmental Panel on Climate Change (IPCC TAR) [Prather et al., 2001]; the lifetime with respect to all sinks is 9.9 years for "Best Guess" as compared with 8.4 years for the IPCC TAR. The strength of the OH sink is determined by the rate constant for the CH_4 + OH reaction, the temperature distribution, and the concentrations and distributions of OH and CH_4, all with associated uncertainties. Assuming that the concentration of OH is the dominant source of uncertainty, the "Low OH" inversion implies a mean concentration for OH 27% lower than the estimate by Spivakovsky et al. [2000], outside the uncertainty range quoted in that study, but only 10% lower than and within the uncertainty range quoted by Prinn et al. [2001]. The average OH concentration for the "High OH" case is 17% higher than Spivakovsky et al. and 44% higher than Prinn et al., outside the uncertainty ranges of both. The average OH for the "Best Guess" is 7% lower than Spivakovsky et al. and 13% higher than Prinn et al. The OH concentrations for the three inversions translate into lifetimes for MCF with respect to tropospheric OH 42% longer, 10% shorter, and 12% longer than that of Prinn et al., respectively, and 49% longer, 5% shorter, and 18% longer than that of Spivakovsky et al. [2000]. Note that it is unclear why the OH averages of Spivakovsky et al. and Prinn et al. are so different; most

likely, the discrepancy can be attributed at least in part to differences in the vertical and horizontal resolutions of the models.

Table 1 includes results from some previous methane inversion studies. Hein et al. [1997] and Houweling et al. [1999] estimated larger values for the OH sink than the result from our "Low OH" inversion, even though they allowed the OH sink to be adjusted by the inversion. We believe that the larger value obtained by Houweling et al. can be attributed to the fact that they assumed an extremely small a priori error for the OH sink, 5% (2σ). Regarding the Hein et al. study, use of large a priori estimates with small uncertainties for the sources (e.g. 270 ± 50 Tg for wetlands) may have resulted in the large OH sink in order to satisfy mass balance.

The source estimates for swamps, biomass burning, and biofuels differ significantly between the "Low OH" and "High OH" inversions, with values being higher for the "High OH" case. The difference is particularly large for swamps: 80 Tg for "Low OH" and 230 Tg for "High OH" as compared to the a priori value of 195 Tg based on the work of Walter et al. [2001a]. Total wetland emissions, including bogs and tundra, are 107 Tg, 258 Tg, 176 Tg, and 260 Tg for "Low OH", "High OH", "Best Guess", and a priori, respectively. Bottom-up estimates of total wetland emissions in the literature, excluding Walter et al., range from 80 to 156 Tg [references in Walter et al., 2001a; Cao et al., 1998]. Walter et al. suggest that their estimate may be anomalously high because the wetland sites used to calibrate their process-based model exhibit high emissions that may not be representative of large regions. Only the estimate in the "Low OH" inversion lies within the range of most bottom-up estimates, but that for the "Best Guess" is close to the upper end of those estimates. The spatial distributions for swamps, biomass burning, biofuels, and tropospheric OH are similar, with maxima in the tropics. Examination of the averaging kernel, or model resolution function, for the OH parameter, included in Table 5, reveals a high degree of anti-correlation between the OH and biomass burning parameters and some anti-correlation of the swamps and biofuels parameters with the OH sink. The correlations indicate that the a posteriori strengths of the tropical sources depend on the strength of the OH sink. These sources are small in the "Low OH" inversion, balancing low OH, and large in the "High OH" inversion, balancing high OH. The correlations imply that these tropical sources are not well constrained by the available observations.

The results for the "High OH" inversion are similar to those of the "Low OH" case for animals + fossil + waste - soil sink, bogs + tundra, and rice paddies, with values for all of these except for the rice source lower than the a priori. The a posteriori values for the (animals + fossil + waste - soil sink) parameter are 30 Tg (15%), 19 Tg (9%), and 23 Tg (12%) lower than the a priori for the "Low OH", "High OH", and "Best Guess" inversions, respectively. These are sizable decreases, although the a posteriori values still lie within the large a priori uncertainty range. The decreases in the bogs + tundra parameter are even larger in relative (and absolute) terms, 59%, 57%, and 58% for the three inversions, and place the estimates outside the a priori uncertainty range. The increases in the rice paddy source are 40%, 45%, and 46%, with the a posteriori strengths lying within the a priori uncertainty range. The agreement among the three inversions suggests that the estimates for these sources are robust. Furthermore, the reductions in uncertainty obtained through the inversion procedure are large for these parameters--~88% for animals + fossil + waste – soil sink, ~65% for rice, and ~76% for bogs + tundra for all three inversions, signifying that the parameters are well constrained by the observations.

Figure 3 presents comparisons of a priori and a posteriori ("Low OH" and "High OH") model CH_4 concentrations with observations at selected sites. It can be seen that the a posteriori agreement between model and observations is improved. A notable improvement is the

latitudinal gradient—the a priori concentrations are generally too high in the extratropical Northern Hemisphere (NH) and too low in the rest of the world. The latitudinal gradient can be seen more clearly in Figure 4, in which latitudinal profiles of annual mean concentration are plotted. In both the "Low OH" and "High OH" cases, decreases in the animal, fossil fuel, waste, bogs, and tundra sources, located primarily in mid- and high-latitudes of the Northern Hemisphere, help to eliminate the positive model bias at these latitudes. In "Low OH", a decrease in OH contributes to an increase in concentrations of CH_4 in the tropics and in the extratropical SH. In "High OH", where the OH sink is not allowed to change, tropical sources, especially swamps, are increased significantly to raise the concentrations in the tropics and the extratropical SH. Included in Table 4 is the percentage of global emissions occurring in the SH for each of the budgets. As may be seen, the "Low OH" budget has a relatively small proportion of emissions in the SH, while the "High OH" budget has a larger proportion in the SH. This result reflects the fact that 57% of global emissions from swamps and 44% of global emissions from biomass burning occur in the SH, while the proportion for most of the other sources is 25% or less. An interesting implication of these results is that the discrepancy between bottom-up (80-156 Tg) and top-down (e.g. 190-230 Tg in Hein et al. [1997]) estimates for wetlands can be explained perhaps by the overestimate of OH in the top-down budgets, which requires high tropical wetland emissions for mass balance.

Agreement between model and observed amplitudes of the seasonal cycle is improved also with the "Low OH" inversion, especially in the mid- and high-latitude Southern Hemisphere (SH), e.g. at Easter Island, Cape Grim and Palmer Station, and at certain high-latitude NH sites, including Baltic Sea and Station M. In contrast, the amplitude of the seasonal cycle is overestimated in these regions with the "High OH" simulation. According to results of our tagged simulations of individual sources/sinks, the seasonal cycle of CH_4 in these regions is shaped largely by OH. Hence, the overestimate of the seasonal cycle further supports the idea that OH is too high in the "High OH" case. The chi-squared (cost function) value provides a quantitative measure of the goodness of fit to the observations and to the a priori constraints, with the expected value for a satisfactory retrieval being 1. The values of χ^2 for the three main inversions, included in Table 4, indicate that the model fit is improved in all three cases, with the "Low OH" and "Best Guess" a posteriori budgets fitting the constraints better than the "High OH" budget.

A variety of tests was implemented to assess the sensitivity of the inversion results to our methods and assumptions. For example, polluted continental sites (all located in the Northern Hemisphere) were excluded in one inversion in order to assess the influence of possible inaccuracies in the model's simulation of pollution episodes. The OH sink was included as an inversion parameter. The results, shown in Table 4, are generally similar to those of the standard "Low OH" inversion, other than a higher estimate for the (animals + fossil + waste – soil sink) parameter and a lower estimate for the rice parameter. The smaller a priori-to-a posteriori decrease in the (animals + fossil + waste – soil sink) parameter relative to the standard inversion can be explained by the fact that the decrease is driven largely by an a priori overestimate of annual mean CH_4 at high-latitude Northern Hemisphere sites, especially continental ones. The lower estimate for the rice parameter relative to the standard inversion is driven perhaps by mass balance requirements, considering that the estimates for the (animals + fossil + waste – soil sink) parameter and swamps are higher than in the standard inversion. Overall, possible inaccuracies in model simulation of pollution episodes do not affect significantly the main conclusions from our inverse analysis.

We examined results also for a different year, 1993. The parameter estimates are generally similar to those for 1994, suggesting that they are robust. A significant difference is that the estimate for the OH sink for 1993 is 16 Tg higher than that for 1994. This may indicate that the inverse calculation captures the effect of Mt. Pinatubo on OH concentrations in 1993. (The effect of Pinatubo on OH is discussed further in Section 3.4.4.) Another difference is that the estimate for emissions from rice paddies is 24 Tg higher than for 1994. An actual change of this magnitude from one year to the next is unlikely. The estimate for 1993 is probably less accurate than for 1994, since the South China Sea shipboard observations, which help to constrain the source from rice paddies, are lacking for the former year.

Other sensitivity tests included use of a different set of a priori source estimates, compiled by the EPA [2001; 2002] (see Table 1 for these source estimates); exclusion of sites located close to other sites in order to minimize possible effects of correlation of observation errors; use of a different spatial and seasonal distribution for OH (from Spivakovsky et al. [2000]); and a decrease in the a priori uncertainty for the OH parameter by a factor of 2. In all cases, the a posteriori budgets (not shown in Table 4) are similar to that obtained with the standard "Low OH" inversion.

Our analysis suggests that EDGAR values for landfills, animals, and fossil fuels, which are based largely on the default methodologies in the *Revised 1996 IPCC Guidelines* [IPCC, 1997], may be high, although a large uncertainty range is attached to these estimates. There is additional evidence in the literature supporting this conclusion. Bogner and Matthews [2003] developed time series for emissions from landfills that scaled the emissions to energy consumption rather than population, used more realistic assumptions for the CH_4 potential of waste and oxidation within landfills, and included data for gas recovery. They found global emissions for 1996, 48 Tg, lower than the 57 Tg estimated on the basis of the IPCC default method. For the source from animals, the default IPCC approach overestimates the contribution from cattle since all animals are treated as full-sized adults, despite the fact that a significant portion are immature and emit less CH_4 [E. Matthews, personal communication]. Our results for the anthropogenic sources, especially oil and gas and animals, are more in line with those from the global inventory compiled by the EPA [2001; 2002] (Table 1). The EPA included for many sources IPCC "Tier 2" and "Tier 3" estimates, which involve detailed methods and country-specific emission factors rather than the default methods adopted in "Tier 1" estimates. Our rice paddy source however is higher than the EPA's result, as is the case for the comparison with EDGAR. Recent bottom-up estimates for this source, including those of EDGAR and EPA, are significantly lower than earlier estimates. For example, earlier estimates include 63 Tg (for Asia alone) [Neue et al., 1990; Bachelet and Neue, 1993], and 60 Tg [Olivier et al., 1999], while the latest EDGAR estimate is 39 Tg, the value from the EPA is 30 Tg, and Denier van der Gon [2000] estimated 39 Tg. Reasons for the decrease in estimated emissions include use of a lower factor for the conversion of soil-returned carbon to net emitted CH_4 [Denier van der Gon, 2000], and measurements over a whole growth period rather than on a few individual days [Sass et al., 1999]. Our inversion results, with a best guess of 56.6 ± 8.4 Tg, suggest that the recent estimates may be too low.

3.4. Interannual Simulations

3.4.1. Model Evaluation

Time series of results for both the "Low OH" and "High OH" cases are compared with measurements from selected CMDL sites in Figure 5; the "Best Guess" (not shown) gives results

intermediate between these two cases. The "High OH" simulation adopts the original OH fields from the CO study, while for the "Low OH" simulation the original OH fields are scaled by a uniform factor of 0.623 in accordance with the "Low OH" inversion result. The model agrees well with the observations in general, capturing much of the temporal and spatial variability. Sites affected by frequent pollution episodes contributed by local emissions, such as Tae-ahn Peninsula, Mace Head, and Barrow, are more difficult to simulate with the coarse-resolution model. Values of r^2 for model-observation correlations and the average model bias are included in Table 6. Values of r^2 lie between 0.70 and 0.99 for many sites, confirming that the model captures much of the temporal variability; values are lower for sites impacted by local emissions. Values are generally higher for the "Low OH" run than the "High OH" run, especially in the Southern Hemisphere, reflecting the more accurate simulation of the seasonal cycle in the former case. The high values for correlation between model and observations largely reflect the similarity in the seasonal cycles and long-term trend. When the average seasonal cycle and trend (harmonic and quadratic fit) are removed from the time series, r^2 values drop to 0.15-0.50 for many sites. Correlations are still significant at a 99% confidence level for many of the sites, as indicated in Table 6. The average model biases are generally close to zero, but higher in NH mid- and high-latitude source regions and lower in the SH for the "High OH" simulation than for "Low OH".

Plots of the instantaneous growth rate time series are shown in Figure 6. The agreement between model (both "Low OH" and "High OH") and observations is satisfactory in general. The agreement is particularly good in the SH (e.g. South Pole, Palmer Station, Cape Grim, Pacific Cruises 20S, Samoa, Ascension Island, and Seychelles) and at Barbados, Midway, and Alert. Growth rates are binned into global and semi-hemispheric averages in Figure 7. (We included all the sites listed in Table 3 that spanned the period January 1988-December 1997, internal gaps being acceptable. The smoothed, deseasonalized time series were averaged for each bin, then the instantaneous growth rate was computed.) The agreement between model and observations is excellent for the Southern Hemisphere, though not as good for the Northern Hemisphere. The "Low OH" simulation tends to underestimate the amplitude of the interannual oscillations, while the "High OH" simulation tends to overestimate it.

Warwick et al. [2002] conducted a global simulation of CH_4 in which they accounted for interannual variability in meteorology but used the same sources and sinks each year. They used ECMWF meteorological analyses for 1980-1998. Their model captured a portion of the observed variability in growth rate, indicating that meteorology contributes to interannual variability of CH_4 trends on local and even global scales. They suggested that changes in the rates of mixing between the hemispheres, between the tropics and extratropics, and between the surface and higher altitudes could influence the global-average lifetime of CH_4 as well as force the growth rates in different regions in opposite directions. Table 7 presents a comparison of values of r^2 for model-observation correlations in detrended growth rates from Warwick et al. and the present study. Our values for r^2 are larger or about the same as those of Warwick et al. for all of the sites they reported, implying that inclusion of variability in sources and sinks improves the agreement between model and observations. (It should be noted though that they used a different time period, 1984-1998, from that in our study in calculating their correlations.) Furthermore, our simulation with interannual variability in sources and sinks captures on a global basis the anomalous growth rates observed during 1991-1993, while the simulation of Warwick et al. [2002] fails to do so. Model results for 1991-1993 are discussed in detail below in Section 3.4.4.

Results for the vertical distribution of CH_4 were evaluated using aircraft measurements, as shown in Figure 8. Model profiles are in good agreement with the observations for most of the geographic regions. The model captures the general decrease in concentrations with altitude in the NH and the increase with altitude in the SH, indicating that the large-scale mixing of more polluted air from the NH and cleaner air from the SH is simulated correctly. Agreement of the model with the PEM-West A observations and the Japan Coast observations in PEM-West B is less satisfactory. This can be attributed probably to the small sample sizes and large standard deviations, particularly for Southeastern China and Japan in PEM-West A.

3.4.2. Causes of the Slowdown in Methane Growth

We show below that the slowdown in methane growth over the past decade can be attributed to a combination of slower growth of sources and increases in OH. The global total source, sink, and model net source (i.e. growth rate), are displayed for each year of the "Low OH" and "High OH" interannual simulations in Figure 9a, along with the "Best Guess" and observed net source. It can be seen that all three simulations capture the observed general decline in growth rate over the period. Figure 9b, which breaks the methane budget down into individual components, shows that most of the sources were nearly constant. This contrasts with earlier decades, when many of the anthropogenic sources had been increasing steadily, as suggested by socioeconomic statistics [references in Table 2]. This finding is consistent with the hypothesis by Khalil and Shearer [1993] that leveling off of emissions from the animal and rice sources may be responsible for the decline in CH_4 growth, but extends the hypothesis to include other sources such as coal mining and gas venting/flaring as well.

Global mean OH (shown deseasonalized and smoothed in Figure 10) exhibits a positive trend of 0.64%/year over the period, further enhancing the decline in CH_4 growth. The OH trend is driven primarily by a negative trend in the overhead column of O_3 that was used to calculate OH [Duncan et al., 2003c]. Duncan et al. show that column O_3 decreased at all latitudes between 1988 and 1997. In a calculation in which the total O_3 column was held constant at 1988 levels, the trend in OH is much smaller, +0.16%/year (Figure 10). This result is consistent with the finding by Logan et al. [1981] and Spivakovsky et al. [2000] that OH is highly sensitive to changes in the O_3 column but less sensitive to changes in other chemical variables. A large upward jump in OH between 1995 and 1996 is apparent for the fixed O_3 column simulation, suggesting that the change from GEOS-1 to GEOS-STRAT meteorological input may have led to a spurious trend in OH. However, even if the jump in 1995 were removed from the time series, there remains a significant upward trend in OH overall for the standard simulation.

We did not account for interannual variability of a number of variables that affect OH, such as the concentrations of NO_x, tropospheric O_3, NMHCs, and aerosols in the stratosphere (direct scattering effects) and troposphere. There is no evidence for a trend in tropospheric O_3 in Northern mid-latitudes during this period [Logan et al., 1999]. Tropical surface O_3 data do not show a trend either [Oltmans et al., 1998]. Also, while emissions of NO_x and NMHCs were increasing in Asia, they were decreasing in North America and Europe. Despite the uncertainties in our calculation of the OH trend, the positive sign of the trend is supported by some previous studies. A 3-D CTM simulation by Karlsdottir and Isaksen [2000] found a positive trend in OH (+0.43%/year for 1980-1996, with OH increasing monotonically throughout the period). They accounted for interannually varying NO_x, CO, CH_4, and NMHCs, but not column O_3. Dentener et al. [2003] calculated a trend of +0.26%/year for 1979-1993 using a 3-D CTM with interannually varying O_3 columns as well as NO_x, CO, and hydrocarbon emissions. The trend of

column ozone in the tropics is largely influenced by the 11-year solar cycle [e.g. WMO, 2003]; there is no long-term trend when the solar cycle is removed. Hence, the trend calculated for global OH will depend significantly on the years selected for the analysis. A maximum in solar flux at 10.7 cm (a proxy for the solar cycle) happens to occur near the beginning of our analysis period (around 1990; see Figure 4-5 in WMO, 2003), corresponding to a maximum in tropical column ozone, and a minimum occurs around 1997. The peak-to-trough difference in tropical ozone of around 4% contributes to the large positive trend in OH obtained in this study.

In contrast to the bottom-up analyses, Prinn et al. [2001] inferred a negative trend in OH of ~-1.3%/year during 1988-1997 using MCF observations. They reported a positive trend in OH of ~+1.5%/year from 1979 to 1989 followed by a negative trend of ~-1.9%/year from 1989 to 2000. However, a calculation by Krol and Lelieveld [2003] demonstrates that such large interdecadal swings in OH could be avoided if a small portion of the MCF emissions for the mid-1980s through early 1990s based on McCulloch and Midgley [2001] were shifted to earlier and later periods. The authors suggested that unreported stockpiling of MCF in anticipation of the phase-out instituted by the 1990 London Amendment to the Montreal Protocol, or a larger proportion of MCF falling into the "slow-use" category, could have caused a significant delay between sales and emissions, consistent with a shifting of emissions to the later period. Further support for this hypothesis was provided by Krol et al. [2003] and Barnes et al. [2003], who found that emissions of MCF from developed countries appear to have been higher than reported officially after 1995, possibly due to gradual usage of stockpiled supplies, illegal production or sale, and/or slower release to the atmosphere of packaged or landfilled chemical than previously thought. Krol et al. [2003] inferred significant MCF emissions in Europe from aircraft measurements in 2000, a year for which official estimates are close to zero. They pointed out that these emissions from Europe alone would be enough to eliminate the negative OH trend for the 1990s calculated by Prinn et al. [2001]. Similarly, the estimates of Barnes et al. [2003] for MCF emissions during 1996-1998 are significant, based on continuous measurements capturing pollution episodes in the northeastern U.S., and imply continuing emissions for several years thereafter. In conclusion, MCF observations cannot provide reliable information on OH trends until a definitive estimate of MCF emissions becomes available.

3.4.3. Other Possible Causes of the Slowdown in CH_4 Growth

There are a number of factors that might contribute to the slowdown in CH_4 growth that were not taken into account in our simulations. A decline in emissions from rice paddies in China due to a transition from continuous flooding to intermittent flooding practices has been proposed by Li et al. [2002]. Their modeling study suggests that emissions may have been about 5 Tg lower in 2000 than 1980 (cf. a decrease of about 20 Tg y^{-1} in the observed CH_4 growth rate between 1988 and 1997 as shown in Figure 9a). Also, as noted above, studies have suggested that deposition of sulfate may have suppressed CH_4 emissions from wetlands and rice paddies due to competition for substrate from sulfate reducing bacteria (e.g. Gauci et al., 2002; van Bodegom et al., 2001). In addition, adoption of modern varieties of rice and switching from the use of organic fertilizer to the use of mineral fertilizer may have slowed the rise in emissions from rice paddies, although data on the extent of organic fertilizer use is scarce [Denier van der Gon, 2000, 1999]. We did not account for emissions mitigation efforts that began around 1990 particularly in the U.S. and Western Europe [D. Kruger, personal communication; Olivier, 2002]. Emission factors for coal mines and landfills may have decreased since then as a result of increased capture and utilization of CH_4 from those sources. Olivier [2002] estimated that CH_4

recovery from coal mines may have amounted to 1 Tg in 1990, and 2 Tg in 1995. In addition, there has been a shift from underground to surface mining of coal in some places, particularly the U.S., Western Europe, and the FSU, which lowers the emission factors [EPA, 2001; Olivier, 2002]. Global coal mining emissions decreased by 3 Tg/yr from 1990-1995 according to the EDGAR inventory [Olivier, 2002] and by 2 Tg/yr from 1990-1995 in the EPA inventory [EPA, 2002], in contrast to the 1 Tg/yr increase estimated with our simpler calculation.

Despite neglect of possible decreases in emission factors over the simulation period, the modeled trend of CH_4 agrees with the observed. Possible errors in calculated trends for certain sources and sinks, for example an overestimate of the trend in OH resulting from an unphysical jump between the GEOS-1 and GEOS-STRAT model versions, could be compensating for the neglect of decreases in emission factors.

3.4.4. 1991-1993 Anomaly

As shown in Figure 9a, the model reproduces the shapes of most of the observed fluctuations in CH_4 growth rate, including, most noticeably, the sharp decrease between 1991 and 1992. The "Best Guess" simulation reproduces the magnitude of this decrease accurately; it is underestimated in the "Low OH" case and overestimated with "High OH". The similarity in the pattern of interannual variations among the three simulations demonstrates that the conclusions regarding the interannual variability of CH_4 do not depend on the inversion results. Figure 9b reveals that the interannual variability of the CH_4 budget during the analysis period was driven mainly by wetlands and by removal of CH_4 by reaction with tropospheric OH. The strength of the OH sink was in turn determined largely by global OH concentrations rather than by CH_4 concentrations, as can be seen from the strong correlation between global average OH in Figure 10 and the strength of the OH sink in Figure 9b.

For the "Best Guess" simulation, the wetlands source decreased by 20 Tg from 1991 to 1992, and remained relatively low in 1993. There was an increase in the removal rate of CH_4 by reaction with OH of 9 Tg from 1991 to 1992, and an increase of another 10 Tg in 1993, the year with minimum column ozone and maximum global average OH in this period (Figure 10). The fossil fuel source, on the other hand, changed little between 1991 and 1993. There was a decrease of 4 Tg in the biomass burning source from 1991 to 1992, and the source remained low in 1993 (the estimate for 1993 is less reliable since the TOMS AI data were interrupted from May onward). This change in the biomass burning source is smaller than the decrease of 20 Tg hypothesized by Lowe et al. [1997] to explain the CH_4 growth rate anomaly.

The fluctuations in wetland emissions and OH are related to the eruption of Mt. Pinatubo in June 1991. The sulfate injected into the stratosphere reflected a significant amount of incoming solar radiation for more than a year, contributing to a negative anomaly in temperatures at the surface in 1992-1993 [Hansen et al., 1992; Dutton and Christy, 1992, McCormick et al., 1995]. The globally averaged anomaly was -0.5°C in 1992, and -0.7°C in the high-latitude NH. Also, precipitation was below average in many regions. A larger fractional decrease in emissions from 1991 to 1992 occurred for bogs and tundra than for swamps in our model (28%, or 8 Tg, vs. 7%, or 12 Tg), reflecting the larger temperature decrease and greater sensitivity to precipitation changes at high northern latitudes. The increase in particulate sulfate in the stratosphere contributed also to enhanced loss of stratospheric ozone, leading to anomalously low values in 1992-1993 [e.g. WMO, 1999]. The effect of the change in ozone can be seen in Figure 10, where the pronounced maximum in OH during 1993 is absent from the simulation in which the O_3 columns were fixed at 1988 levels.

Another feature of the CH_4 data is the anomously high growth rate in the latter part of 1991. Our model omits the radiative effects of the enhanced sulfate aerosol and short-lived SO_2 (residence time ~31 days) in the stratosphere that were proposed by Dlugokencky et al. [1996] as the cause of the positive growth rate anomaly. This may account for our underestimate of the magnitude of the anomaly (Figure 9a).

The anomalous growth rates during 1991-1993 are simulated remarkably well by the model at most of the CMDL sites, as shown in Figure 6. In Figure 7, the agreement between model and observations is good during 1991-1993 for all four semi-hemispheres; there are some discrepancies in the magnitude of the growth rate, but the timing of the fluctuations is accurate. The model-observation comparisons confirm our hypothesis that changes in wetland emissions and OH concentrations after the eruption of Mt. Pinatubo can account for the anomalous behavior of CH_4 during 1991-1993. A notable feature of the growth rate curves is that the negative anomaly occurs earlier in the Northern Hemisphere, peaking in mid-1992, while it peaks in late 1992-early 1993 in the Southern Hemisphere. This reflects the fact that the eruption of Mt. Pinatubo had a more immediate impact on emissions from northern high-latitude bogs, affecting global OH concentrations later (OH peaked in 1993). Also, the long time-scale for interhemispheric exchange results in a lag between the signal of the decrease in bog emissions as observed in the Northern Hemisphere and the detection of the effect in the Southern Hemisphere.

4. Discussion

The economies of Eastern Europe and the FSU are expected to recover over the next decade or two [EIA, 2002; EPA, 2001]. It is likely that the economic growth will be accompanied by increases in fossil fuel production and consumption, growth in animal populations, enhancement in production of organic waste, and increases in other CH_4 sources. Population and economic growth in other parts of the world are likely to contribute to additional growth in future CH_4 emissions. A report published by the U.S. Department of Energy's Energy Information Administration (EIA) forecasts an increase in energy consumption from coal, oil, and natural gas between 1998 and 2020 of 113% for developing countries and 38% for developed countries, corresponding to a global average of 65% [EIA, 2002]. Increases in per capita income often lead to higher consumption of meat and other animal products [Tanzer, 1995; Sedik, 1993], resulting in larger domesticated animal populations. A large trend has already occurred in developing countries like China and Brazil. The EPA [2001; 2002] projects steady increases in global anthropogenic CH_4 emissions over the next two decades, associated particularly with the oil and natural gas, animal, and waste sources. Total anthropogenic emissions are projected to increase by about 50% between 1995 and 2020 in developing countries, about 5% in developed countries, and about 40% for the world. These emissions are based on "Business as Usual" scenarios estimated by individual nations as part of their National Communications to the U.N. Framework Convention on Climate Change. The data from the EIA and the EPA suggest there is potential for significant growth in CH_4 emissions over coming decades.

We have seen that a positive trend in OH has partially masked the effects of increasing CH_4 emissions on the growth of atmospheric CH_4 over the period of our analysis. There is reason to expect that the positive trend in OH will not continue indefinitely, and in fact that it is likely to reverse. Since stratospheric O_3 appears to be a dominant contributor to recent OH trends, a recovery of the O_3 layer from the decline of recent decades would result in a significant

decrease in OH. The largest declines in O_3 have occurred at high and mid-latitudes, reflecting chemical destruction by anthropogenic chlorine and bromine in addition to the impact of changes in atmospheric dynamics [WMO, 2003]. About 25% of the global OH sink for CH_4 occurs at latitudes poleward of 32°N and S according to our model. As discussed above, the decrease in O_3 in the tropical stratosphere over the period 1988-1997 reflects the influence of the 11-year solar cycle. Therefore, a recovery in tropical O_3 would be expected to occur over subsequent years as part of this cycle, promoting growth of atmospheric CH_4. A recovery of the CH_4 growth rate is not apparent from the most recent observations from the CMDL network, which indicate that the growth rate has remained low through 2002, with the exception of 1998, when growth rates were as high as those in the 1980s [E. Dlugokencky, personal communication; Dlugokencky et al., 2001]. The lack of recovery can be explained perhaps by the fact that the actual ozone column in the tropics did not increase consistently between 1997 and 2002; it increased during 1998-1999 but decreased thereafter [WMO, 2003]. In addition, animal populations, natural gas production, and coal production either continued to decrease or increased only slightly in Eastern Europe and the former Soviet Union between 1997 and 2001, indicating that an economic recovery for this region has yet to occur.

In the IPCC Third Assessment Report [Prather et al., 2001], global average OH is calculated to decrease by 10%-20% over the next century for all but one of the emissions scenarios tested. The lifetime of CH_4 increases accordingly. The modeled decrease in OH is due to large increases in CO, CH_4, and VOC emissions, which dominate over effects of higher emissions of NO_x. These results illustrate the potential for increases in pollutant emissions to lead to a decrease in OH, enhancing thereby future growth of CH_4 concentrations.

Altogether, our model results and the possible future trajectories for sources and sinks suggest that the recent slowdown in CH_4 growth may be temporary. In fact, there is potential for large increases in CH_4 concentration in the future with a significant impact on climate and tropospheric O_3 pollution, if human activities proceed along a "business-as-usual" trajectory. Fortunately, technically and economically feasible methods are available to moderate the growth in CH_4 emissions, and indeed have been implemented already in some locations as noted above. In some of these instances, mitigation of greenhouse warming was not the primary motivation for reducing emissions. In China for example, mid-season drainage of rice paddies was intended to conserve water and increase yields, and reduction of CH_4 emissions arose as an ancillary benefit [Li et al., 2002]. But if awareness grows of the importance of CH_4 as a greenhouse gas and a precursor for tropospheric ozone, mitigation methods may be systematized and applied on a larger scale, reducing, perhaps even halting, future growth of CH_4.

5. Conclusions

In this study, a 3-D CTM accounting for interannual variations in emissions, transport, and chemical sinks was employed in a combination of top-down and bottom-up approaches to analyze trends of CH_4 over the past decade. The interhemispheric mixing in the model was verified to be accurate, in contrast to some previous CH_4 inversion studies. We found that the slowdown in the growth rate of CH_4 over the past decade can be explained by a slowdown in the growth of emissions compared to earlier decades in combination with a secular increase in OH from 1988 to 1997. The economic downturn in Eastern Europe and the former Soviet Union since the early 1990s has had a significant effect on the global growth of emissions. The significant trend in OH was driven mainly by a decrease in column ozone, related to the influence of the 11-year solar cycle in the tropics and ozone depletion at higher latitudes. The

positive trend for OH inferred here agrees with results from previous bottom-up studies, but differs from the negative trend derived using MCF for the period 1988-1997 in a top-down study by Prinn et al. [2001]. Observations suggest that MCF emissions from the U.S. and Europe have been higher than reported officially for the 1990s; accounting for the unreported emissions would eliminate the negative trend in OH inferred by Prinn et al. Further work is needed to reconcile the bottom-up and top-down estimates for the OH trend.

A number of previous studies suggested that concentrations of CH_4 may be approaching a steady-state and may even decrease in the next few decades, implying that CH_4 will not contribute much further to increasing radiative forcing of climate. Results of the present study suggest that the recent slowdown in CH_4 growth may be temporary. Economic recovery in Eastern Europe and the former Soviet Union, continued population and economic growth in other parts of the world, and a reversal of the recent positive trend in OH would promote more rapid growth of CH_4.

With respect to the long-standing question of what caused the anomalously low growth rates of CH_4 observed during 1992-1993, the present study attributes a dominant influence to fluctuations in wetland emissions and OH concentrations following the eruption of Mt. Pinatubo. Lower temperatures and precipitation suppressed wetland emissions, while reductions in stratospheric ozone, peaking in 1993, led to enhanced production of OH in the troposphere. The contribution to the growth anomaly from these distinct factors is reflected in a lag in the growth anomaly in the SH relative to the NH. During the period 1988-1997 as a whole, variations in the wetland source and OH account for most of the interannual fluctuations in the CH_4 growth rate.

We presented a best-guess budget for year 1994. The tropospheric mean OH concentration for this budget, based on an inversion using observations of methyl chloroform, corresponds to a lifetime for CH_4 with respect to all sinks of 9.9 years, longer than the 9.3 years reported in Prinn et al. [2001] and the 8.4 years assumed in the IPCC TAR [Prather et al., 2001]. The smaller OH sink of the present study allows for a lower wetland source than previous inversion studies; an overestimate of OH may explain the discrepancy between previous top-down and bottom-up estimates for the wetland source. The inversion results reported here suggest that the estimates in the EDGAR inventory, largely based on IPCC default methods, may be too high for several of the anthropogenic sources (animals, fossil fuels, and landfills and waste water). The estimate of Walter et al. [2001a] for bogs and tundra also appears to be high. Emissions from rice paddies, on the other hand, are greater than indicated by recent bottom-up estimates. The inversion results from the present study do not support the possibility of unusually high leakage from FSU natural gas pipelines, which is suggested by anecdotal evidence [e.g. Dlugokencky et al., 1994a]. It is important to note however that our inversion approach does not shed light on emissions processes or regional contributions for individual sources. Further work needs to be carried out to understand the discrepancies between the results from this study and previous estimates for rice paddies and other sources.

The addition of long-term observations in the tropics that exhibit stronger source signals would help constrain the strengths of the swamp, biomass burning, and termite sources, which cannot currently be estimated reliably by an inversion approach. New sites immediately downwind of other important source regions such as the natural gas producing areas of West Siberia would help to constrain individual anthropogenic sources. Satellite observations of CH_4, which might become available in the near future, would also be useful in this regard. Future studies should examine in further detail the effects on recent CH_4 trends of changing emission factors due, for example, to shifts from underground to surface coal mining and changes in water

management practices in rice agriculture. Multi-year 3-D simulations of the isotopic composition of CH_4 may provide additional insight into trends in sources. The utility of such simulations might hinge however on the establishment of long-term measurement sites in addition to currently existing ones [Lowe et al., 1997; Francey et al., 1999; Quay et al, 1999; Miller et al., 2002; Tyler et al., 1999], especially sites close to source regions.

Acknowledgements

This work was supported by an NSF Graduate Research Fellowship and a Bertram J. and Barbara B. Cohn Dissertation Fellowship to J.S.W., an NSF grant ATM-9320078, a NASA NAG5-11431, and an NSF ATM-0236501. The authors thank Dylan Jones, Paul Palmer, and Parvadha Suntharalingam for generously providing help and advice on the inverse modeling, and Yaping Xiao, Rosemarie Yevich, Brendan Field, Andrew Fusco, and Yuxuan Wang for their contributions to various aspects of the model development and data analysis. We engaged in helpful discussions with Clarissa Spivakovsky, Philip Cameron-Smith, Bernadette Walter, Ed Dlugokencky, Elizabeth Scheehle, Dale Allen, Prasad Kasibhatla, Mat Evans, Daniel Jacob, and Arlene Fiore.

References

Andreae, M.O., and P. Merlet, Emission of trace gases and aerosols from biomass burning, *Global Biogeochemical Cycles, 15*, 955-966, 2001.

Bachelet, D., and H.U. Neue, Methane emission from wetland rice areas of Asia, *Chemosphere, 26*, 219-237, 1993.

Barnes, D.H., S.C. Wofsy, B.P. Fehlau, E.W. Gottlieb, J.W. Elkins, G.S. Dutton, and S.A. Montzka, Urban/industrial pollution for the New York City-Washington, D. C., corridor, 1996-1998: 2. A study of the efficacy of the Montreal Protocol and other regulatory measures, *J. Geophys. Res., 108*(D6), 4186, doi: 10.1029/2001JD001117, 2003.

Bekki, S., K.S. Law, and J.A. Pyle, Effect of ozone depletion on atmospheric CH_4 and CO concentrations, *Nature, 371*, 595-597, 1994.

Bekki S. and K.S. Law, Sensitivity of the atmospheric CH_4 growth rate to global temperature changes observed from 1980 to 1992, *Tellus, 49B*, 409-416, 1997.

Bey, I., D.J. Jacob, R.M. Yantosca, J.A. Logan, B.D. Field, A.M. Fiore, Q. Li, H. Liu, L.J. Mickley, and M.G. Schultz, Global modeling of tropospheric chemistry with assimilated meteorology: Model description and evaluation, *J. Geophys. Res., 106,* 23,073-23,095, 2001.

Blunier, T., J.A. Chappelaz, J. Schwander, J.-M. Barnola, T. Desperts, B. Stauffer, and D. Raynaud, Atmospheric methane, record from a Greenland ice core over the last 1000 year, *Geophysical Research Letters, 20*, 2219-2222, 1993.

Bogner, J., and E. Matthews, Global methane emissions from landfills: New methodology and annual estimates 1980-1996, *Global Biogeochemical Cycles, 17(2)*: art. no. 1065, 2003.

Cao, M.K., K. Gregson, and S. Marshall, Global methane emission from wetlands and its sensitivity to climate change, *Atmospheric Environment, 32*, 3293-3299, 1998

Cicerone, R.J., and R.S. Oremland, Biogeochemical aspects of atmospheric methane, *Global Biogeochemical Cycles, 2,* 299-327, 1988.

Denier van der Gon, H.A.C., Changes in CH_4 emission from rice fields from 1960 to 1990s - 1. Impacts of modern rice technology, *Global Biogeochemical Cycles, 14,* 61-72, 2000.

Denier van der Gon, H.A.C., Changes in CH_4 emission from rice fields from 1960 to 1990s - 2. The declining use of organic inputs in rice farming, *Global Biogeochemical Cycles, 13,* 1053-1062, 1999.

Dentener, F., M. van Weele, M. Krol, S. Houweling, and P. van Velthoven, Trends and inter-annual variability of methane emissions derived from 1979-1993 global CTM simulations, *Atmospheric Chemistry and Physics, 3*, 73-88, 2003.

Dlugokencky, E.J., K.A. Masarie, P.M. Lang, P.P. Tans, L.P. Steele, and E.G. Nisbet, A dramatic decrease in the growth rate of atmospheric methane in the northern hemisphere during 1992, *Geophysical Research Letters, 21*, 45-48, 1994a.

Dlugokencky, E.J., L.P. Steele, P.M. Lang, and K.A. Masarie, The growth rate and distribution of atmospheric methane, *J. Geophys. Res., 99*, 17,021-17,043, 1994b.

Dlugokencky, E.J., E.G. Dutton, P.C. Novelli, P.P. Tans, K.A. Masarie, K.O. Lantz, and S. Madronich, Changes in CH_4 and CO growth rates after the eruption of Mt. Pinatubo and their link with changes in tropical UV flux, *Geophys. Res. Lett., 23*, 2761-2764, 1996.

Dlugokencky, E.J., K.A. Masarie, P.M. Lang, and P.P. Tans, Continuing decline in the growth rate of the atmospheric methane burden, *Nature, 393*, 447-450, 1998.

Dlugokencky, E.J., B.P. Walter, K.A. Masarie, P.M. Lang, and E.S. Kasischke, Measurements of an anomalous global methane increase during 1998, *Geophys. Res. Lett., 28*, 499-502, 2001.

Duncan, B., D. Portman, I. Bey and C. Spivakovsky, Parameterization of OH for Efficient Computation in Chemical Tracer Models, *J. Geophys. Res., 105*, 12,259-12,262, 2000.

Duncan, B. N., R. V. Martin, A. C. Staudt, R. Yevich, J. A. Logan, Interannual and Seasonal Variability of Biomass Burning Emissions Constrained by Satellite Observations, *J. Geophys. Res., 108(D2*), 4040, doi:10.1029/2002JD002378, 2003a.

Duncan, B.N., J.A. Logan, I. Bey, R.V. Martin, D.J. Jacob, R.M. Yantosca, P.C. Novelli, N.B. Jones, C.P. Rinsland, Model study of the variability and trends of carbon monoxide (1988-1997), 1, Model formulation, evaluation, and sensitivity, *J. Geophys. Res.* to be submitted 2003b.

Duncan, B. N., J. A. Logan, Model analysis of variability and trends of carbon monoxide from 1998 to 1997. 2. Trends and regulating factors, *J. Geophys. Res,* to be submitted, 2003c.

Dutton, E.G., and J.R. Christy, Solar radiative forcing at selected locations and evidence for global lower tropospheric cooling following the eruptions of El Chichon and Pinatubo, *Geophys. Res. Lett., 19*, 2313-2316, 1992.

EIA, *International Energy Outlook 2002*, Report No. DOE/EIA-0484(2002), Energy Information Administration, Office of Integrated Analysis and Forecasting, U.S. Dept. of Energy, Washington, D.C., March 2002.

EPA, *Non-CO2 Greenhouse Gas Emissions from Developed Countries: 1990-2010*, Report No. EPA-430-R-01-007, U.S. Environmental Protection Agency, Washington, D.C., 2001.

EPA, International Analysis of Methane and Nitrous Oxide Abatement Opportunities: Report to Energy Modeling Forum, Working Group 21, U.S. Environmental Protection Agency, Washington, D.C., December 2002.

Etheridge, D.M., L.P. Steele, R.J. Francey, and R.L. Langenfelds, Atmospheric methane between 1000 A.D. and present: Evidence of anthropogenic emissions and climatic variability, *J. Geophysical Research, 103*, 15,979-15,993, 1998.

Francey, R.J., M.R. Manning, C.E. Allison, S.A. Coram, D.M. Etheridge, R.L. Langenfelds, D.C. Lowe, and L.P. Steele, A history of $\delta^{13}C$ in atmospheric CH_4 from the Cape Grim Air Archive and Antarctic firn air, *J. Geophysical Research, 104*, 23,631-23,643, 1999.

Fung, I., J.John, J. Lerner, E. Matthews, M. Prather, L.P. Steele, and P.J. Fraser, Three-dimensional model synthesis of the global methane cycle, *J. Geophysical Research, 96*, 13,033-13,065, 1991

Gauci, V., N. Dise, and D. Fowler, Controls on suppression of methane flux from a peat bog subjected to simulated acid rain sulfate deposition, *Global Biogeochemical Cycles, 16*, 993-1004, 2002.

Gupta, M., S. Tyler, and R. Cicerone, Modeling atmospheric $\delta^{13}CH_4$ and the causes of recent changes in atmospheric CH_4 amounts, *J. Geophysical Research, 101,* 22,923-22,932, 1996.

Hansen, J., A. Lacis, R. Ruedy, and M. Sato, Potential climate impact of Mount Pinatubo eruption, *Geophys. Res. Lett., 19*, 251-218, 1992.

Hansen, J., M. Sato, R. Ruedy, A. Lacis, and V. Oinas, Global warming in the twenty-first century: An alternative scenario, *Proc. Natl. Acad. Sci., USA, 97*, 9875-9880, 2000.

Hein, R., P.J. Crutzen, and M. Heimann, An inverse modeling approach to investigate the global atmospheric methane cycle, *Global Biogeochemical Cycles,* 11, 43-76, 1997

Herman, J. R., P. K. Bhartia, O. Torres, C. Hsu, C. Seftor, and E. Celarier, Global distribution of UV-absorbing aerosols from Nimbus 7/TOMS data, *J. Geophys. Res., 102*, 16,911–16,922, 1997.

Hogan, K.B. and R.C. Harriss, Comment on 'A dramatic decrease in the growth rate of atmospheric methane in the Northern Hemisphere during 1992; by E.J. Dlugokencky et al., *Geophys. Res. Lett., 21*, 2445-2446, 1994.

Houweling, S., T. Kaminski, F. Dentener, J. Lelieveld, and M. Heimann, Inverse modeling of methane sources using the adjoint of a global transport model, *J. Geophys. Res., 104*, 26,137-16,160, 1999.

Hsu, N. C., J. R. Herman, P. K. Bhartia, C. J. Seftor, O. Torres, A. M. Thompson, J. F. Gleason, T. F. Eck, and B. N. Holben, Detection of biomass burning smoke from TOMS measurements, *Geophys. Res. Lett*., *23*, 745–748, 1996.

IPCC, *IPCC Guidelines for National Greenhouse Gas Inventories*. 3 volumes: Vol. 1, Reporting Instructions; Vol. 2, Workbook; Vol. 3, Reference Manual. Intergovernmental Panel on Climate Change, United Nations Environment Programme, Organization for Economic Co-operation and Development, International Energy Agency. Paris, France, 1997.

Jacob, D. J., M. J. Prather, S. C. Wofsy, and M. B. McElroy, Atmospheric distribution of ^{85}Kr simulated with a general circulation model, *J. Geophys. Res., 92,* 6614-6626, 1987.

Jones, D.B.A., K.W. Bowman, P.I. Palmer, J.R.Worden, D.J. Jacob, R.N. Hoffman, I. Bey, and R.M. Yantosca, Potential of observations from the Tropospheric Emission Spectrometer to constrain continental sources of carbon monoxide, *J. Geophys. Res.*, submitted, 2003.

Jöckel, P., R. von Kuhlmann, M.G. Lawrence, B. Steil, C.A.M. Brenninkmeijer, P.J. Crutzen, P.J. Rasch, and B. Eaton, On a fundamental problem in implementing flux-form advection schemes for tracer transport in 3-dimensional general circulation and chemistry transport models, *Q. J. R. Meteorol. Soc., 127*, 1035-1052, 2001.

Karlsdóttir, S. and I. S. A. Isaksen, Changing methane lifetime: Possible cause for reduced growth, *Geophys. Res. Lett., 27,* 93-96, 2000.

Khalil, M.A.K. and R. Rasmussen, Decreasing trend of methane: unpredictability of future concentrations, *Chemosphere, 26*, 803-814, 1993.

Khalil, M.A.K. and M.J. Shearer, Sources of Methane: An Overview, in *Atmospheric Methane: Sources, Sinks, and Role in Global Change*, edited by M.A.K. Khalil, NATO ASI Series, Vol. 13, 1993

Krol, M., P. Jan van Leeuwen and J. Lelieveld, Global OH trend inferred from methylchloroform measurements, *J. Geophysical Research, 103,* 10,697-10,711, 1998.

Krol M.C., J. Lelieveld, D.E. Oram, G.A. Sturrock, S.A. Penkett, C.A.M. Brenninkmeijer, V. Gros, J. Williams, and H.A. Scheeren, Continuing emissions of methyl chloroform from Europe, *Nature*, *421* (6919): 131-135, 2003.

Krol, M., and J. Lelieveld, Can the variability in tropospheric OH be deduced from measurements of 1,1,1,-trichloroethane (methyl chloroform)?, *J. Geophys. Res., 108*(D3), 4125, doi:10.1029/2002JD002423, 2003.

Lacroix, A.V., Unaccounted-for sources of fossil and isotopically-enriched methane and their contribution to the emissions inventory: A review and synthesis, *Chemosphere, 26*, 507-557, 1993.

Law, K.S. and E.G. Nisbet, Sensitivity of the CH_4 growth rate to changes in CH_4 emissions from natural gas and coal, *J. Geophysical Research, 101*, 14,387-14,397, 1996.

Lelieveld, J. P.J. Crutzen, and F.J. Dentener, Changing concentration, lifetime and climate forcing of atmospheric methane, *Tellus, Ser. B, 50*, 128-150, 1998.

Lerner, J. E. Matthews and I. Fung, Methane emission from animals: a global high resolution data base, *Global Biogeo. Cycles, 2*, 139-156, 1988.

Li, C., J. Qiu, S. Frolking, X. Xiao, W. Salas, B. Moore III, S. Boles, Y. Huang, and R. Sass, Reduced methane emissions from large-scale changes in water management of China's rice paddies during 1980-2000, *Geophys. Res. Lett., 29(20),* 1972, doi:10.1029/2002GL015370, 2002.

Lobert, J.M., W. C. Keene, J. A. Logan, and R. Yevich, Global chlorine emissions from biomass burning: the reactive chlorine emissions inventory, *J. Geophys. Res., 104,* 8373-8390, 1999.

Logan, J. A., M. J. Prather, S. C. Wofsy, and M. B. McElroy, Tropospheric chemistry: A global perspective, *J. Geophys. Res., 86,* 7210-7254, 1981.

Logan, J.A., I.A. Megretskaia, A.J. Miller, G.C. Tiao, D. Choi, L. Zhang, R.S. Stolarski, G.J. Labow, S.M. Hollandsworth, G.E. Bodeker, H. Claude, D. De Muer, J.B. Kerr, D.W. Tarasick, S.J. Oltmans, B. Johnson, F. Schmidlin, J. Staehelin, P. Viatte, and O. Uchino, Trends in the vertical distribution of ozone: a comparison of two analyses of ozonesonde data, *J. Geophys. Res., 105,* 26,373-26399, 1999.

Lowe, D.C., C.A.M. Brenninkmeijer, G.W. Brailsford, K.R. Lassey, A.J. Gomez, and E.G. Nisbet, Concentration and ^{13}C records of atmospheric methane in New Zealand and Antarctica: Evidence for changes in methane sources, *J. Geophysical Research, 99,* 16,913-16,925, 1994.

Lowe, D.C., M.R. Manning, G.W. Brailsford, and A.M. Bromley, The 1991-1992 atmospheric methane anomaly: Southern Hemisphere ^{13}C decrease and growth rate fluctuations, *Geophys Res Lett, 24*, 857-860, 1997

Marks, C.J., and C.D. Rodgers, A retrieval method for atmospheric composition from limb emission measurements, *J. Geophys. Res., 98*, 14,939-14,953, 1993.

Marland, G., T. A. Boden, R. J. Andres, A. L. Brenkert, and C. A. Johnston, Global, Regional, and National Fossil Fuel CO_2 Emissions, Trends Online: A Compendium of Data on Global Change. Oak Ridge National Laboratory, U.S. Department of Energy, Oak Ridge, Tennessee, http://cdiac.ESD.ORNL.GOV/trends/emis/em_cont.htm, 2001.

Martin, R. V., D. J. Jacob, J. A. Logan, I. Bey, R. M. Yantosca, A. C. Staudt, Q. Li, A. M. Fiore, B. N. Duncan, H. Liu, P. Ginoux, and V. Thouret, Interpretation of TOMS observations of tropical tropospheric ozone with a global model and in-situ observations, *J. Geophys. Res*., *107(D18)*, 4351, 10.1029/2001JD001480, 2002.

Matthews, E., Global vegetation and land use: new high-resolution data bases for climate studies, *J. Climate Appl. Meteorol., 22*, 474-487, 1983.

Matthews, E., and I. Fung. Methane Emissions from Natural Wetlands: Global Distribution, Area, and Ecology of Sources, *Global Biogeochemical Cycles, 1,* 61-86, 1987.

Matthews, E., I. Fung, and J. Lerner, Methane emissions from rice cultivation: geographic and seasonal distribution of cultivated areas and emissions, *Global Biogeochemical Cycles, 5*, 3-24, 1991.

McCormick, M.P., L.W. Thomason, and C.R. Trepte, Atmospheric effects of the Pinatubo eruption, *Nature, 373*, 399-404, 1995.

McCulloch, A., and P.M. Midgley, The history of methyl chloroform emissions: 1951-2000, *Atmos. Environ., 35*, 5311-5319, 2001.

Midgley, P.M. and A. McCulloch, The production and global distribution of emissions to the atmosphere of 1,1,1-trichloroethane (methyl chloroform), *Atmos. Environ., 29*, 1601-1608, 1995.

Miller J.B., K. A. Mack, R. Dissly, J.W.C. White, E.J. Dlugokencky, and P.P. Tans, Development of analytical methods and measurements of C-13/C-12 in atmospheric CH_4 from the NOAA Climate Monitoring and Diagnostics Laboratory global air sampling network*, J. Geophys. Res. 107(D13):*4178, 2002.

Neue, H.U., P. Becker-Heidmann, and H.W. Scharpenseel, Organic matter dynamics, soil properties, and cultural practices in rice lands and their relationship to methane production, in: *Soils and the Greenhouse Effect*, edited by A.F. Bouwman, pp. 457-466, John Wiley, New York, 1990.

Olivier, J.G.J., A.F. Bouwman, J.J.M. Berdowski, C. Veldt, J.P.J. Bloos, A.J.H. Visschedijk, C.W.M. van der Maas, P.Y.J. Zandveld, Sectoral emission inventories of greenhouse gases for 1990 on a per country basis as well as on 1° x 1°, *Environmental Science and Policy, 2*, 241-263, 1999.

Olivier, J.G.J., On the Quality of Global Emission Inventories: Approaches, Methodologies, Input Data and Uncertainties, Thesis Utrecht University, 2002.

Oltmans, S.J., A.S. Lefohn, H.E. Scheel, J.M. Harris, H. Levy, I.E. Galbally, E.G. Brunke, C.P. Meyer, J.A. Lathrop, B.J. Johnson, D.S. Shadwick, E. Cuevas, F.J. Schmidlin, D.W. Tarasick, H. Claude, J.B. Kerr, O. Uchino, and V. Mohnen, Trends of ozone in the troposphere, *Geophys. Res. Lett., 25*, 139-142, 1998.

Palmer, P. I., D. J. Jacob, D. B. A. Jones, C. L. Heald, R. M. Yantosca, J. A. Logan, G. W. Sachse, and D. G. Streets, Inverting for emissions of carbon monoxide from Asia using aircraft observations over the western Pacific , *J. Geophys. Res.*, accepted, 2003.

Prather, M., M. McElroy, S. Wofsy, G. Russell, and D. Rind, Chemistry of the global troposphere: Fluorocarbons as tracers of air motion, *J. Geophys. Res., 92*, 6579-6613, 1987.

Prather, M., D. Ehhalt, F. Dentener, R. Derwent, E. Dlugokencky, E. Holland, I. Isaksen, J. Katima, V. Kirchhoff, P. Matson, P. Midgley, M. Wang: Atmospheric Chemistry and Greenhouse Gases. In: *Climate Change 2001: The Scientific Basis. Contribution of Working Group I to the Third Assessment Report of the Intergovernmental Panel on Climate Change* [Houghton, J.T., Y. Ding, D.J. Griggs, M. Noguer, P.J. van der Linden, X. Dai, K. Maskell, and C.A. Johnson (eds.)]. Cambridge University Press, Cambridge, U.K., and New York, NY, U.S.A., 881 pp., 2001.

Prinn, R. G. et al., Evidence for substantial variations of atmospheric hydroxyl radical in the past two decades, *Science, 292,* 1882-1997, 2001.

Quay, P., J. Stutsman, D. Wilbur, A. Snover, E. Dlugokencky, and T. Brown, The isotopic composition of atmospheric methane, *Global Biogeochemical Cycles, 13*, 445-461, 1999.

Ramaswamy, V., O. Boucher, J. Haigh, D. Hauglustaine, J. Haywood, G. Myhre, T. Nakajima, G.Y. Shi, and S. Solomon: Radiative Forcing of Climate Change. In: *Climate Change 2001: The Scientific Basis. Contribution of Working Group I to the Third Assessment Report of the Intergovernmental Panel on Climate Change* [Houghton, J.T., Y. Ding, D.J. Griggs, M. Noguer, P.J. van der Linden, X. Dai, K. Maskell, and C.A. Johnson (eds.)]. Cambridge University Press, Cambridge, U.K., and New York, NY, U.S.A., 881 pp., 2001.

Ravishankara, A.R., E.J. Dunlea, M.A. Blitz, T.J. Dillon, D.E. Heard, M.J. Pilling, R.S. Strekowski, J.M. Nicovich, and P.H. Wine, Redetermination of the rate coefficient for the reaction of $O(^1D)$ with N_2, *Geophys. Res. Lett., 29*(15), 10.1029/2002GL014850, 2002.

Ridgwell, A.J., S.J. Marshall, and K. Gregson, Consumption of atmospheric methane by soils: A process-based model, *Global Biogeochemical Cycles, 13*, 59-70, 1999.

Rodgers, C.D., *Inverse Methods for Atmospheric Sounding: Theory and Practice*, World Scientific Publishing Co. Pte. Ltd., Singapore, 2000.

Rotman, D.A., C.S. Atherton, D.J. Bergmann, P.J. Cameron-Smith, C.C. Chuang, P.S. Connell, J.E. Dignon, A. Franz, K.E. Grant, D.E. Kinnison, C.R. Molenkamp, D.D. Proctor, and J.R. Tannahill, IMPACT, the LLNL 3-D global atmospheric chemical transport model for the combined troposphere and stratosphere: Model description and analysis of ozone and other trace gases, *J. Geophys. Res.,* submitted, 2003.

Sanderson, M.G., Biomass of termites and their emissions of methane and carbon dioxide: A global database, *Global Biogeochemical Cycles, 10*, 543-557, 1996.

Sass, R.L., F.M. Fisher Jr., A. Ding, and Y. Huang, Exchange of methane from rice fields: national, regional, and global budgets, *J. Geophys. Res., 104*, 26943-26951, 1999.

Schauffler, S.M. and J.M. Daniel, On the effects of stratospheric circulation on trace gas trends, *J. Geophys. Res., 99*, 25,747-25,754, 1994.

Schneider H. R., D. B. Jones, G.-Y. Shi, and M. B. McElroy, Analysis of residual mean transport in the stratosphere. Part I: Model description and comparison with satellite data, *J. Geophys. Res., 105*, 19991-20011, 2000.

Sedik, D.J., Russian Price Reform Eliminates Shortages, Alters Meat Consumption, *Food Review, 16*, 1056327X, September-December, 1993.

Simpson, I.J., D.R. Blake, F.S. Rowland, and T.-Y. Chen, Implications of the recent fluctuations in the growth rate of tropospheric methane, *Geophys. Res. Lett., 29*, 10.1029/2001GL014521, 2002.

Spivakovsky, C. M., J. A. Logan, S. A. Montzka, Y. J. Balkanski, M. Foremen-Fowler, D. B. A. Jones, L. W. Horowitz, C. A. M. Brenninkmeijer, M. J. Prather, S. C. Wofsy, and M. B. McElroy, Three dimensional climatological distribution of tropospheric OH: update and evaluation, *J. Geophys. Res., 105,* 8931-8980, 2000.

Steele, L.P., E.J. Dlugokencky, P.M. Lang, P.P. Tans, R.C. Martin and K.A. Masarie, Slowing down of the global accumulation of atmospheric methane during the 1980s, *Nature, 358,* 313- 316, 1992.

Stevens, C.M., Atmospheric methane, *Chemical Geology, 71*, 11-21, 1988

Tanzer, A., China's ravenous appetite, *Forbes, 156(14)*, 148-151, 1995.

Thoning, K.W., P.P. Tans, and W.D. Komhyr, Atmospheric carbon dioxide at Mauna Loa Observatory 2. Analysis of the NOAA GMCC data, 1974-1985, *J. Geophys., Res., 94*, 8549-8565, 1989.

Torres, O., P. K. Bhartia, J. R. Herman, Z. Ahmad, and J. Gleason, Derivation of aerosol properties from satellite measurements of backscattered ultraviolet radiation: Theoretical basis, *J. Geophys. Res., 103*, 17,099–17,110, 1998.

Tyler, S.C., H.O. Ajie, M.L. Gupta, R.J. Cicerone, D.R. Blake, and E.J. Dlugokencky, Stable carbon isotopic composition of atmospheric methane: A comparison of surface level and free tropospheric air, *J. Geophysical Research, 104*, 13,895-13,910, 1999.

Van Bodegom, P.M., R. Wassman, and T.M. Metra-Corton, A process-based model for methane emission predictions from flooded rice paddies, *Global Biogeochemical Cycles, 15*, 247-263, 2001.

Von Hippel, F., D.H. Albright, and B.G. Levi, Quantities of fissile materials in U.S. and soviet nuclear weapons arsenals, *Rep. PU/CEES 168*, Cent. for Energy and Environ. Stud., Princeton Univ., Princeton, N.J., 1986.

Walter, B.P., Heimann, M., and Matthews, E., Modeling modern methane emissions from natural wetlands, 1. Model description and results, *J. Geophys. Res., 106,* 34,189-34,205, 2001a.

Walter, B.P., Heimann, M., and Matthews, E., Modeling modern methane emissions from natural wetlands, 2. Interannual variations 1982-1993, *J. Geophys. Res., 106*, 34,207-34,219, 2001b.

Wang, Y., J.A. Logan, and D.J. Jacob, Global simulation of tropospheric O_3-NO_x-hydrocarbon chemistry, 2. Model evaluation and global ozone budget, J. *Geophys. Res., 103*, 10,727-10,756, 1998.

Warwick, N.J., S. Bekki, K.S. Law, E.G. Nisbet, and J.A. Pyle, The impact of meteorology on the interannual growth rate of atmospheric methane, *Geophys. Res. Lett., 29*(20), 1947, doi:10.1029/2002GL015282, 2002.

Weiss, W., A. Sittkus, H. Stockburger, and H. Sartorius, Large-scale atmospheric mixing derived from meridional profiles of krypton 85, *J. Geophys. Res., 88*, 8574-8578, 1983.

Whiticar, M.J., Stable isotopes and global budgets, in *Atmospheric Methane: Sources, Sinks, and Role in Global Change*, editted by M.A.K. Khalil, NATO ASI Series, Vol. 13, pp. 138-167, 1993

World Meteorological Organization, (WMO), Scientific assessment of ozone depletion: 1998, Global Ozone Res. Monit. Proj., WMO, Rep. 44, Geneva, 1999.

World Meteorological Organization, (WMO), Scientific assessment of ozone depletion: 2002, Global Ozone Res. Monit. Proj., WMO, Rep. 47, Geneva, 2003.

Yevich, R., and J. A. Logan, An assessment of biofuel use and agricultural waste burning in the developing world, *Global Biogeochem Cycles*, in press, 2003.

Table 1. Comparison of Methane Budget from this Study (in Tg/yr) with Previous Studies

Study	This Study			EPA [2001; 2002]	Fung et al. [1991] (Scenario 7)	Hein et al. [1997] (Scenario 1)	Houweling et al.[1999]
	A Priori		A Posteriori Best Guess				
Budget Year(s)	Various		1994	1995	1980s	1983-1989	1993-1995
Total Source	590		506	--	500	575	505
Natural Sources	285		201	--	140	232	
Wetlands	260	[a]	176	--	115	232	
Bogs and Tundra	65		27	--	35	44	
Swamps	195		149	--	80	188	
Termites	20	[b]	20	--	20	--	
Hydrates	5	[c]	4	--	5	--	
Anthropogenic Sources	306		306	254	350	343	
Oil and Natural Gas	54	[d]	47	42	40	70	
Coal	33	[d]	30	25	35	33	
Landfills and Waste Water	55	[d]	49	55	40	40	
Animals	94	[d]	83	89	80	90	
Rice Paddies	39	[d]	57	30	100	69	
Biomass Burning (incl. Biofuel)	31	[e]	41	10	55	41	
Total Sink	609		492	--	460	541	488
Tropospheric OH	531	[f]	428	--	450	469	451
Stratospheric Loss	40	[g]	30	--	--	44	
Soil Absorption	38	[h]	34	--	10	28	
Net Source	-19		14	--	40	34	17
% Emissions in SH	29		29	--		29	33

[a]Walter et al. [2001a]
[b]Sanderson [1996]
[c]Fung et al. [1991]
[d]EDGAR V3.2, year 1995 [Olivier, 2002]; for animals, we include a 5 Tg contribution from wild animals [Lelieveld et al., 1998]
[e]Duncan et al. [2003a]; Yevich and Logan [2003]
[f]Duncan et al. [2003b]
[g]Hein et al. [1997]
[h]Ridgwell et al. [1999]

Table 2. Variables Used to Model Interannual Variability of Sources

CH_4 Source	**Scaling Variable(s)**	**Source of Data**
Domesticated animals	Animal populations (cattle, water buffalo, sheep)	U.N. Food and Agriculture Organization (FAO) [downloaded in 2001 from http://apps.fao.org/page/collections?subset=agriculture]
Rice paddies	Rice harvest areas	U.N. Food and Agriculture Organization (FAO) [downloaded in 2001 from http://apps.fao.org/page/collections?subset=agriculture]
Natural gas leakage	Natural gas production and consumption	U.S. Energy Information Administration (EIA) [downloaded in 2002 from http://www.eia.doe.gov/emeu/international/gas.html]
Natural gas venting/flaring (oil production)	CO_2 emissions from gas flaring	Carbon Dioxide Information Analysis Center (CDIAC) [Marland et al., 2001]
Coal mining	Coal production	British Petroleum (BP) [downloaded in 2001 from http://www.bp.com/centres/energy/coal/reserves.asp]
Wetlands (swamps, bogs, tundra)	Precipitation and soil temperature	National Center for Environmental Prediction (NCEP); Walter et al. [2001a,b] (emissions responses)
Biomass burning (excluding biofuels)	Total Ozone Mapping Spectrometer (TOMS) Aerosol Index	Hsu et al. [1996], Herman et al. [1997], Torres et al. [1998]; method for estimating emissions in Duncan et al. [2003a]

Table 3. CMDL Measurement Sites Used in This Study

Station Code	Station Name and Location	Latitude	Longitude	Altitude (m)
ALT	Alert, NWT, Canada	82N	63W	210
ASC	Ascension Island, Atlan. Ocean, UK	8S	14W	54
BAL	Baltic Sea, Poland	56N	16E	7
BME	St. David's Head, Bermuda, UK	32N	65W	30
BMW	Southhampton, Bermuda, UK	32N	66W	30
BRW	Barrow, Alaska, USA	71N	157W	11
CBA	Cold Bay, Alaska, USA	55N	163W	25
CGO	Cape Grim, Tasmania, Australia	41S	145E	94
CHR*	Christmas Island, Kiribati	2N	157W	3
CMO	Cape Meares, Oregon, USA	45N	124W	30
EIC	Easter Island, Chile	29S	109W	50
GMI	Guam, Mariana Islands, USA	13N	145E	2
GOZ	Dewejra Point, Gozo, Malta	36N	14E	30
HBA	Halley Bay, Antarctica	76S	26W	10
HUN	Hegyhatsal, Hungary	46N	16E	344
ICE	Heimaey, Iceland	63N	20W	100
ITN	Grifton, North Carolina, USA	35N	77W	505
IZO	Tenerife, Canary Islands, Spain	28N	16W	2300
KEY	Key Biscayne, Florida, USA	26N	80W	3
KUM	Cape Kumukahi, Hawaii, USA	20N	155W	3
MBC	Mould Bay, NWT, Canada	76N	119W	58
MHD	Mace Head, Ireland	53N	10W	25
MID	Sand Island, Midway, USA	28N	177W	4
MLO	Mauna Loa, Hawaii, USA	20N	156W	3397
NWR	Niwot Ridge, Colorado, USA	40N	106W	3475
POC	Pacific Ocean Cruises	35S-30N, every 5°	126-178W	0
PSA	Palmer Station, Antarctica	65S	64W	10
RPB	Ragged Point, Barbados	13N	59W	3
SCS	South China Sea Cruises	3-21N, every 3°	105-114E	0
SEY	Mahe Island, Seychelles	5S	55E	3
SHM	Shemya Island, Alaska, USA	53N	174E	40
SMO	Tutuila, American Samoa, USA	14S	171W	42
SPO	South Pole, Antarctica	90S	25W	2810
STM	Ocean Station M, Norway	66N	2E	7
SYO	Syowa, Antarctica	69S	40E	11
TAP	Tae-ahn Peninsula, Rep. of Korea	37N	126E	20
UTA	Wendover, Utah, USA	39N	113W	1320
UUM	Ulaan Uul, Mongolia	44N	111E	914
WLG	Mt. Waliguan, Qinghai, China	36N	101E	3810
ZEP	Ny-Alesund, Svalbard, Norway and Sweden	79N	12E	475

*Not used in inversions—less than 8 months of data for 1994.

Table 4. Inversion Results

Parameter values and errors in Tg CH_4/yr. Uncertainties are 2σ.

Parameter	**A priori**	**A posteriori (1994)**					
		"Low OH"	**"High OH"**	**"Best Guess"**	**Continental Sites Excluded**	**1993 Inversion**	
Animals + Fossil + Waste - Soil Sink	198 ± 69	168.4 ± 7.8	179.2 ± 8.1	174.9 ± 7.6	187.8 ± 11.3	155.2 ± 8.4	
Termites	19.7 ± 3	19.5 ± 3.0	21.1 ± 3.0	20.3 ± 3.0	19.7 ± 3.0	19.4 ± 3.0	
Soviet Hydrates (72°-80°N, 90°-140°E)	2.5 ± 2.5	4.5 ± 1.2	3.8 ± 1.2	4.2 ± 1.2	3.2 ± 1.6	3.3 ± 1.3	
Zonal Hydrates (80°-88°N)	2.5 ± 2.5	-0.1 ± 0.6	0.0 ± 0.6	-0.1 ± 0.6	-0.1 ± 0.6	-0.2 ± 0.6	
Rice Paddies	38.7 ± 25	54.1 ± 8.4	56.2 ± 8.7	56.6 ± 8.4	39.7 ± 9.3	78.3 ± 11.2	
Bogs + Tundra	65 ± 13	26.5 ± 3.1	27.7 ± 3.1	27.0 ± 3.1	25.6 ± 3.6	29.1 ± 3.5	
Swamps	195 ± 39	79.9 ± 18.6	230.4 ± 9.6	149.2 ± 9.6	96.8 ± 19.8	78.6 ± 18.2	
Biomass Burning	22.1 ± 7	20.4 ± 6.2	28.4 ± 6.0	27.7 ± 5.9	17.4 ± 6.2	23.5 ± 6.5	
Biofuel	9.2 ± 8	9.8 ± 7.1	26.0 ± 9.4	12.8 ± 7.1	9.2 ± 7.5	4.7 ± 7.4	
Tropospheric OH	531 ± 159[a]	336.7 ± 21.2	531[b]	428.3[b]	343.3 ± 23.4	353.2 ± 21.7	
Stratospheric Sink	40 ± 8	32.5 ± 5.2	27.7 ± 5.2	30.4 ± 5.2	39.9 ± 5.3	28.0 ± 5.7	
χ^2		7.14 (a priori); 1.63 (a posteriori)	7.11 (a priori); 2.26 (a posteriori)	17.8 (a priori); 1.76 (a posteriori)			
Total Source	590	414	607	506			
Total Sink	609	402	594	492			
Net Source	-19	14	14	14			
% Emissions in SH	29	24	32	29			
					Prinn et al. [2001]	**Spivakovsky et al. [2000]**	**IPCC TAR [Prather et al., 2001]**
τ_{CH4} , tropospheric OH (years)	9.1	14.4	9.1	11.3	10.1 ± 2.8	--	9.6
τ_{CH4} , all losses (years)	8.1	12.1	8.2	9.9	9.3	--	8.4
Tropospheric Mean OH (10^5 molec cm^{-3})[c]	13.6	8.5	13.6	10.7	9.4 ± 2.6	11.6 ± 1.7	--
$\tau_{CH3CCl3}$, tropospheric OH (years)	5.4	8.5	5.4	6.7	6.0	5.7	--
					Quay et al. [1999]		
Average $\delta^{13}C$ of Source[d]		-53.6‰	-54.0‰	-53.9‰	-53.5‰ ± 2‰		
Average δD of Source[d]		-280.0‰	-287.6‰	-284.3‰	275‰ ± 41‰		
Fossil Fraction[e]		0.19	0.14	0.16	0.18 ± 0.09		

[a] The uncertainty here is higher than the ±15% of Spivakovsky et al. [2000] to account for the 14% higher OH of Duncan et al. [2003b].

[b] Not included as parameter in inversion

[c] Weighted by mass of air

[d] Characteristic isotopic values for individual sources based on Quay et al. [1999], supplemented by Whiticar [1993]

[e] Proportion of very old, ^{14}C-depleted sources (i.e. fossil fuels and methane hydrates)

Table 5. Averaging Kernels (Model Resolution Matrix) for the CH_4 Inversion

	NH	TM	HV	HZ	RH	WN	WS	BB	BF	OH	ST
NH	0.99	0.23	0.33	0	0.02	0.04	-0.01	0.01	0.31	0	0.06
TM	0	0.01	0.01	0	0	0	0	0	0.01	0	0
HV	0	0.01	0.75	0.08	0	0	0	0	0	0	0
HZ	0	0	0.08	0.94	0	0	0	0	0	0	0
RH	0	0.01	-0.13	-0.08	0.89	0.04	0.01	-0.01	0.28	0	-0.17
WN	0	-0.04	0.12	0.06	0.01	0.94	0	-0.01	-0.03	0	0.04
WS	0	0.29	0.14	-0.01	0.02	-0.01	0.77	-0.02	-0.04	-0.01	-0.15
BB	0	0.02	0.01	0.01	0	0	0	0.22	0.06	0	0.01
BF	0	0.04	-0.02	0	0.03	-0.01	0	0.08	0.21	0	0.02
OH	-0.01	-0.41	0.27	0	-0.02	-0.01	-0.22	-0.72	-0.23	0.98	0.16
ST	0	-0.03	0	0	-0.02	0.01	-0.01	0.01	0.02	0	0.58

Key to abbreviations:
NH: animals + waste + fossil - soil sink
TM: termites
HV: Soviet hydrates
HZ: zonal hydrates
RH: rice harvest
WN: northern wetlands (bogs + tundra)
WS: swamps
BB: biomass burning
BF: biofuels
OH: tropospheric OH
ST: stratospheric sink

Each row corresponds to the averaging kernel (model resolution function) for the parameter listed at the left.

Table 6. Comparison of Model and CMDL CH_4 Concentration Time Series

Site	Latitude (degrees)	Longitude (degrees)	r^2 of Correlation		r^2 of Correlation (deseasonalized, detrended)		Average Bias (Model - CMDL) (ppbv)	
			"Low OH" Run	"High OH" Run	"Low OH" Run	"High OH" Run	"Low OH" Run	"High OH" Run
SPO	-90	-25	0.99	0.93	0.50	0.44	7	7
PSA	-65	-64	0.98	0.92	0.40	0.46	6	5
CGO	-41	145	0.97	0.89	0.24	0.19	9	8
pocs20	-20	-174	0.91	0.91	0.16	0.13	5	2
SMO	-14	-171	0.91	0.85	0.28	0.23	7	3
ASC	-8	-14	0.94	0.91	0.33	0.31	0	0
SEY	-5	55	0.80	0.77	0.17	0.17	-4	-6
CHR	2	-157	0.86	0.81	0.09	0.04*	7	8
GMI	13	145	0.88	0.85	0.21	0.20	-4	-5
RPB	13	-59	0.84	0.81	0.18	0.12	7	8
KUM	20	-155	0.90	0.90	0.36	0.35	3	1
MLO	20	-156	0.88	0.81	0.09	0.06	3	3
KEY	26	-80	0.73	0.72	0.18	0.17	2	6
MID	28	-177	0.89	0.89	0.23	0.21	-6	-5
BME	32	-65	0.71	0.73	0.12	0.10	-2	1
BMW	32	-66	0.71	0.74	0.08	0.09	4	8
WLG	36	101	0.22	0.09	0.02*	0.01*	28	41
TAP	37	126	0.03*	0.03*	0.02*	0.02*	-25	-10
NWR	40	-106	0.86	0.84	0.20	0.18	9	12
UUM	44	111	0.44	0.36	0.02*	0.02*	24	40
CMO	45	-124	0.82	0.78	0.05*	0.03*	-12	-9
MHD	53	-10	0.50	0.52	0.37	0.34	-3	2
SHM	53	174	0.82	0.82	0.12	0.12	-14	-9
CBA	55	-163	0.85	0.83	0.09	0.08	-16	-12
STM	66	2	0.82	0.84	0.27	0.27	8	15
BRW	71	-157	0.52	0.52	0.03*	0.01*	-7	0
MBC	76	-119	0.73	0.77	0.19	0.17	4	11
ALT	82	-63	0.73	0.82	0.21	0.21	2	7

*Correlation not significant (p-value > 0.01).

Table 7. Comparison of Model-Observation Correlations in Growth Rate (Detrended) from This Study and Warwick et al. [2002]

	This Study		Warwick et al. [2002]
	"Low OH"	"High OH"	
Site	r^2	r^2	r^2
SPO	0.73	0.59	0.20
PSA	0.68	0.76	
CGO	0.46	0.28	
SMO	0.53	0.4	0.46
ASC	0.68	0.68	0.46
SEY	0.69	0.72	
GMI	0.46	0.45	0.46
RPB	0.51	0.28	
KUM	0.2	0.23	0.27
MLO	0.05	0.04	
KEY	0.35	0.37	0.35
MID	0.67	0.57	
NWR	0.43	0.37	
CMO	0.17	0.13	
CBA	0.24	0.2	0.01
STM	0.35	0.33	0.03
BRW	0	0	0.01
ALT	0.35	0.42	

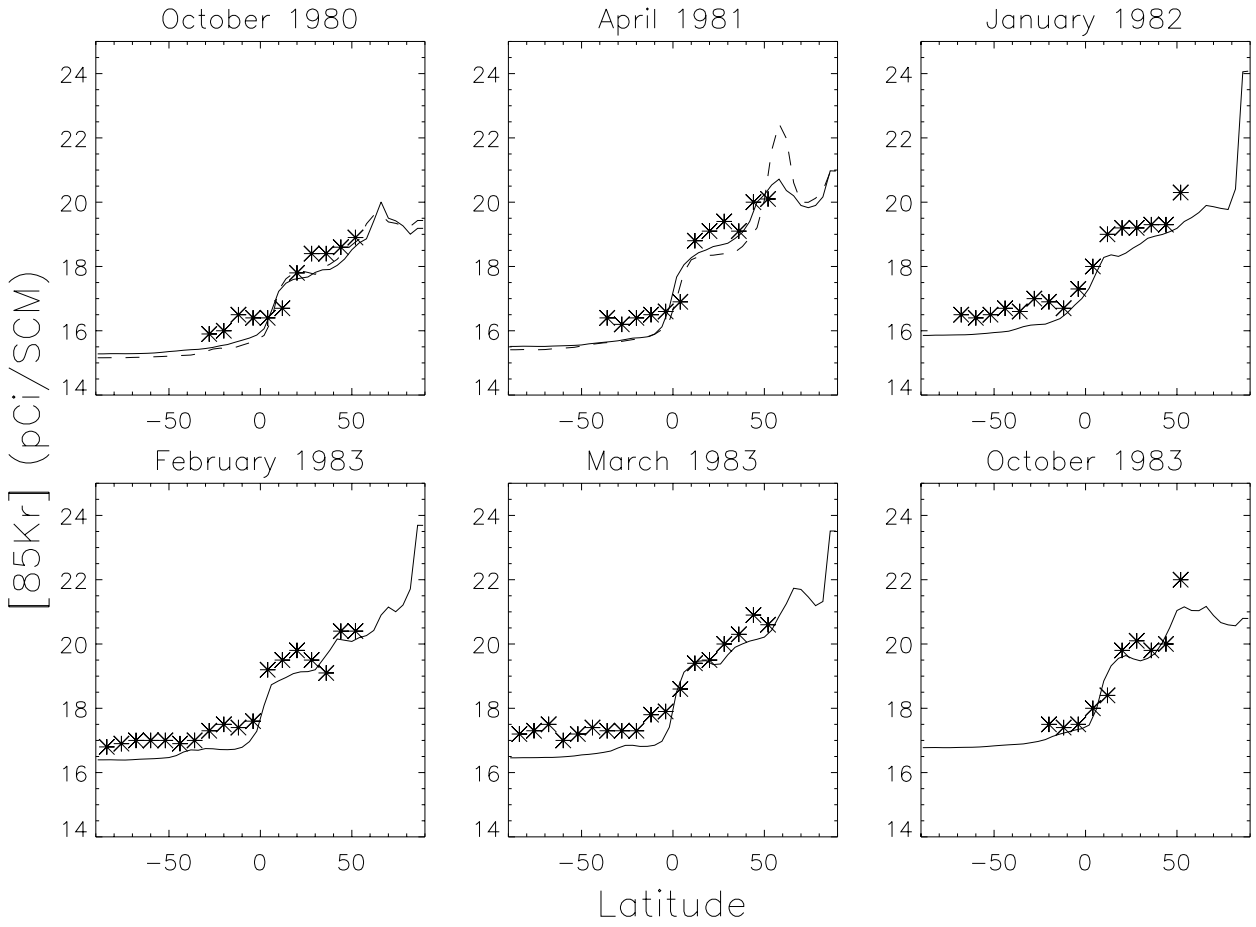

Figure 1. Comparison of model and observed latitudinal distributions of ^{85}Kr in the Atlantic Basin (30°W). Observations (stars) are for 1980-1983. Included are results for GEOS-1 meteorological parameters (1990-1993) with emissions for 1980-1983 (solid lines), and GEOS-STRAT meteorological parameters (1996-1997) with emissions for 1980-1981 (dashed lines). Units are picocuries per cubic meter of air at standard temperature and pressure (pCi/SCM). 1 pCi/SCM equals a mixing ratio of 6.82×10^{-19} vol/vol.

a)

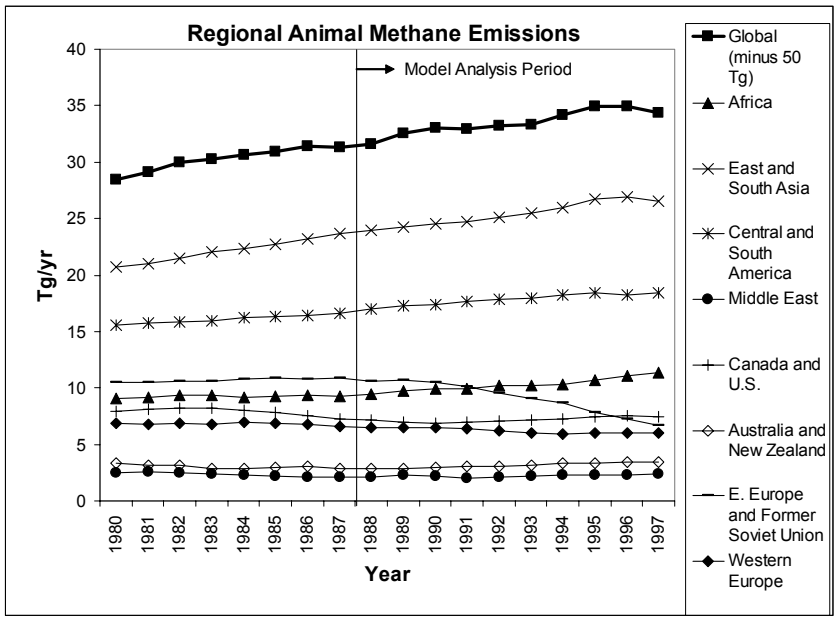

b)

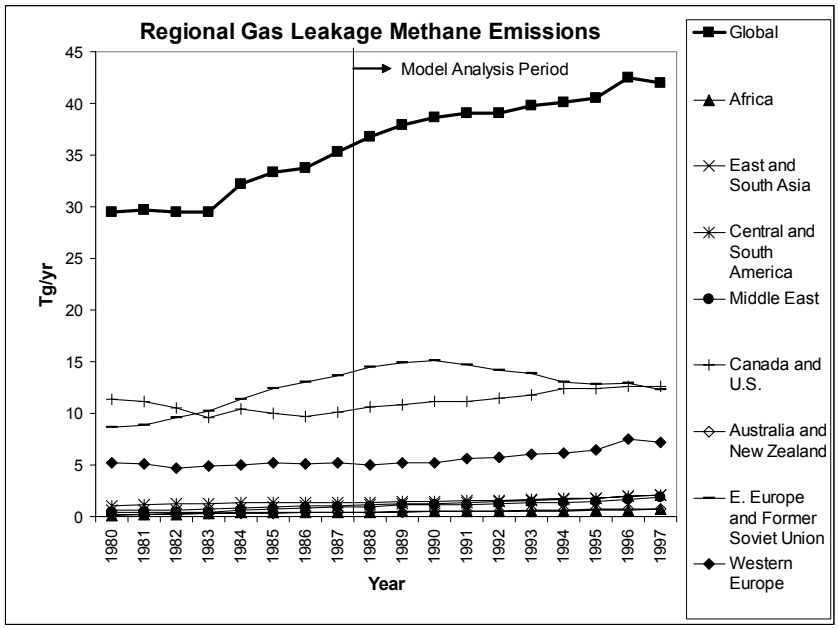

Figure 2. Time series of regional total emissions from (a) ruminant animals; (b) gas leakage; (c) coal mining; and (d) all anthropogenic sources (gas leakage, gas venting, coal, landfills and waste water, ruminants, rice paddies, and biomass burning, including biofuels). Values are included for years prior to the model analysis period to place the model values in context. Note: shown are source strengths derived from the "High OH" inversion (see section 3.3 for an explanation). The anthropogenic source strengths from the "Low OH" inversion are generally similar, except for a biomass burning source that is 48% lower.

c)

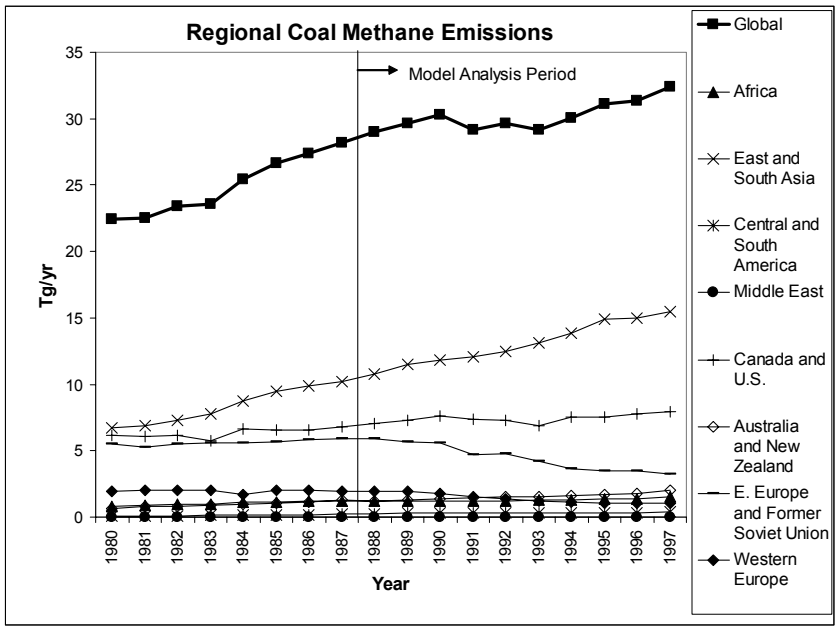

d)

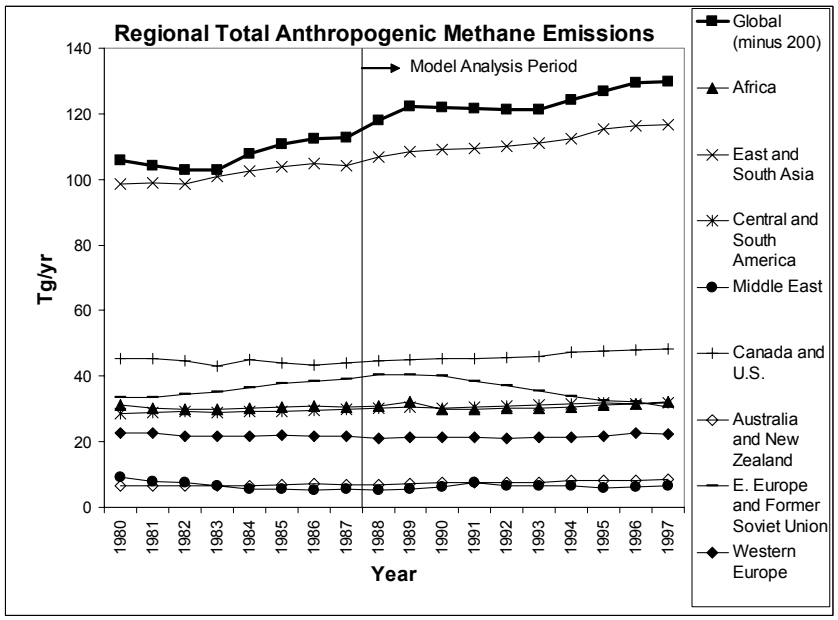

Figure 2. (continued)

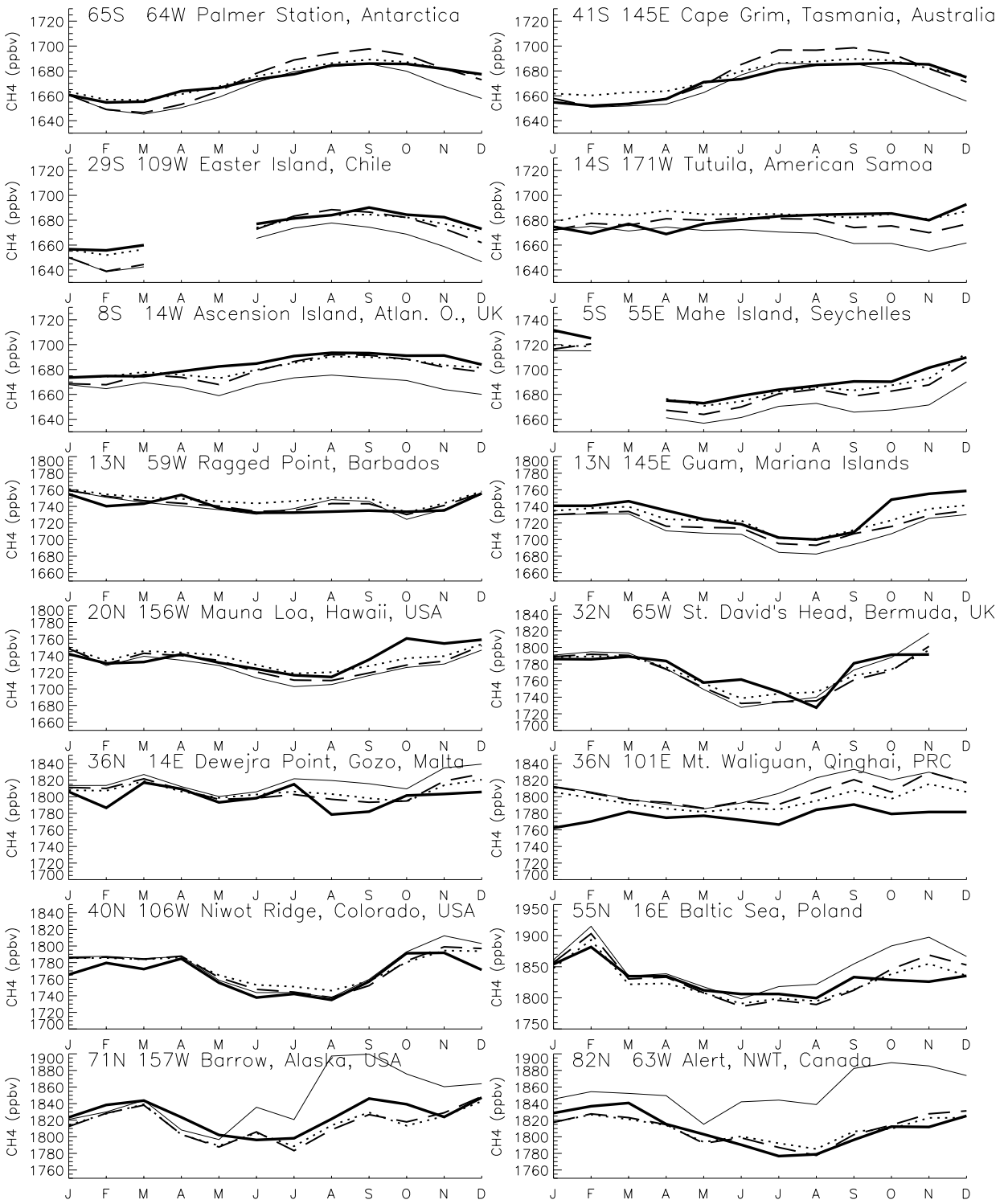

Figure 3. Comparison of model a priori (thin solid lines) and a posteriori ("Low OH" (dotted lines) and "High OH" (dashed lines) inversions) CH_4 monthly means for 1994 with observations (thick solid lines) at selected CMDL sites.

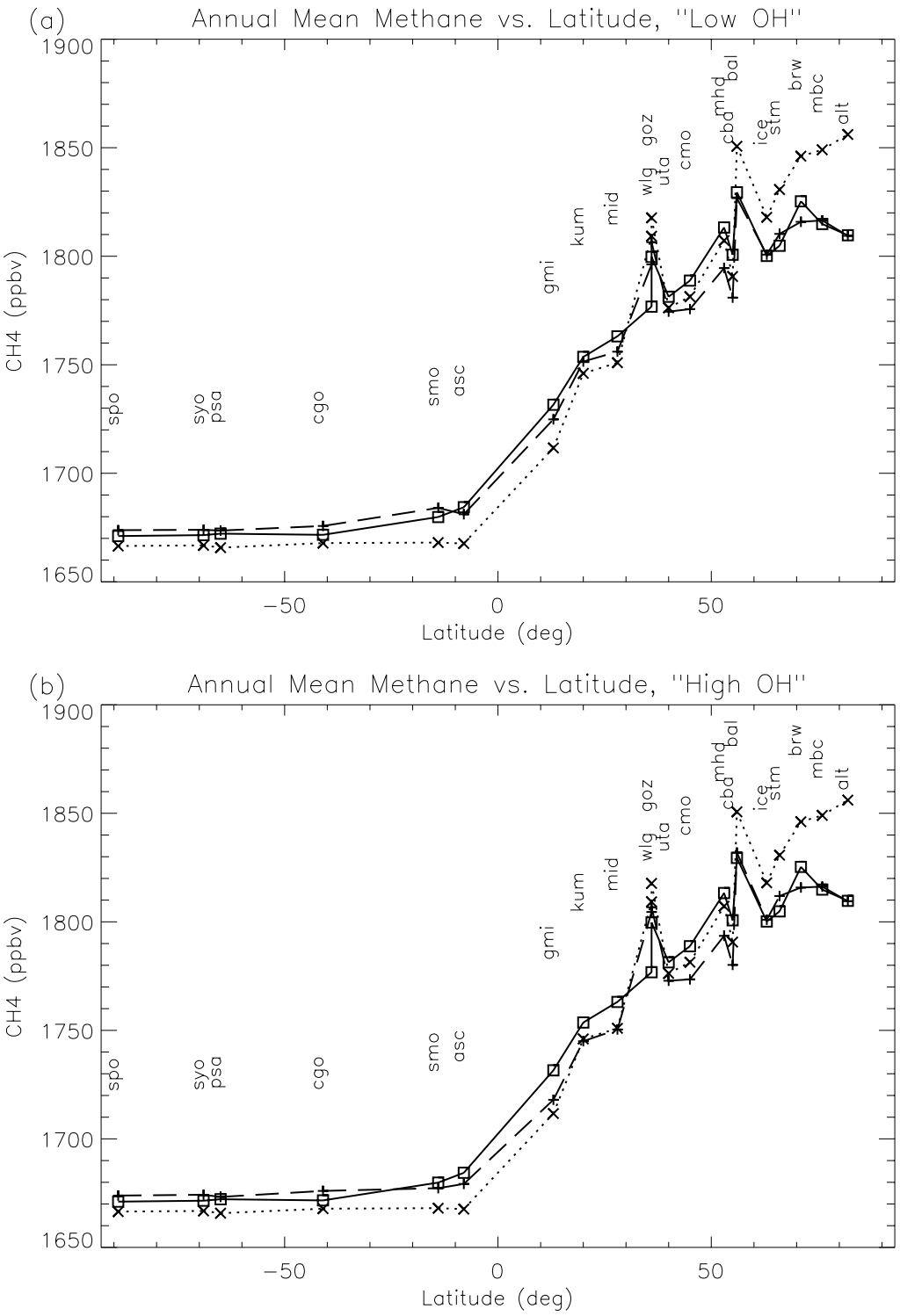

Figure 4. Latitudinal profiles of 1994 annual mean CH_4 for model a priori and a posteriori versus observations at selected CMDL sites. (a) "Low OH" inversion; (b) "High OH" inversion. Squares connected by solid lines represent observations, X's with dotted lines represent the a priori, and +'s with dashed lines represent the a posteriori. CMDL site codes are displayed at a constant offset from the observation values.

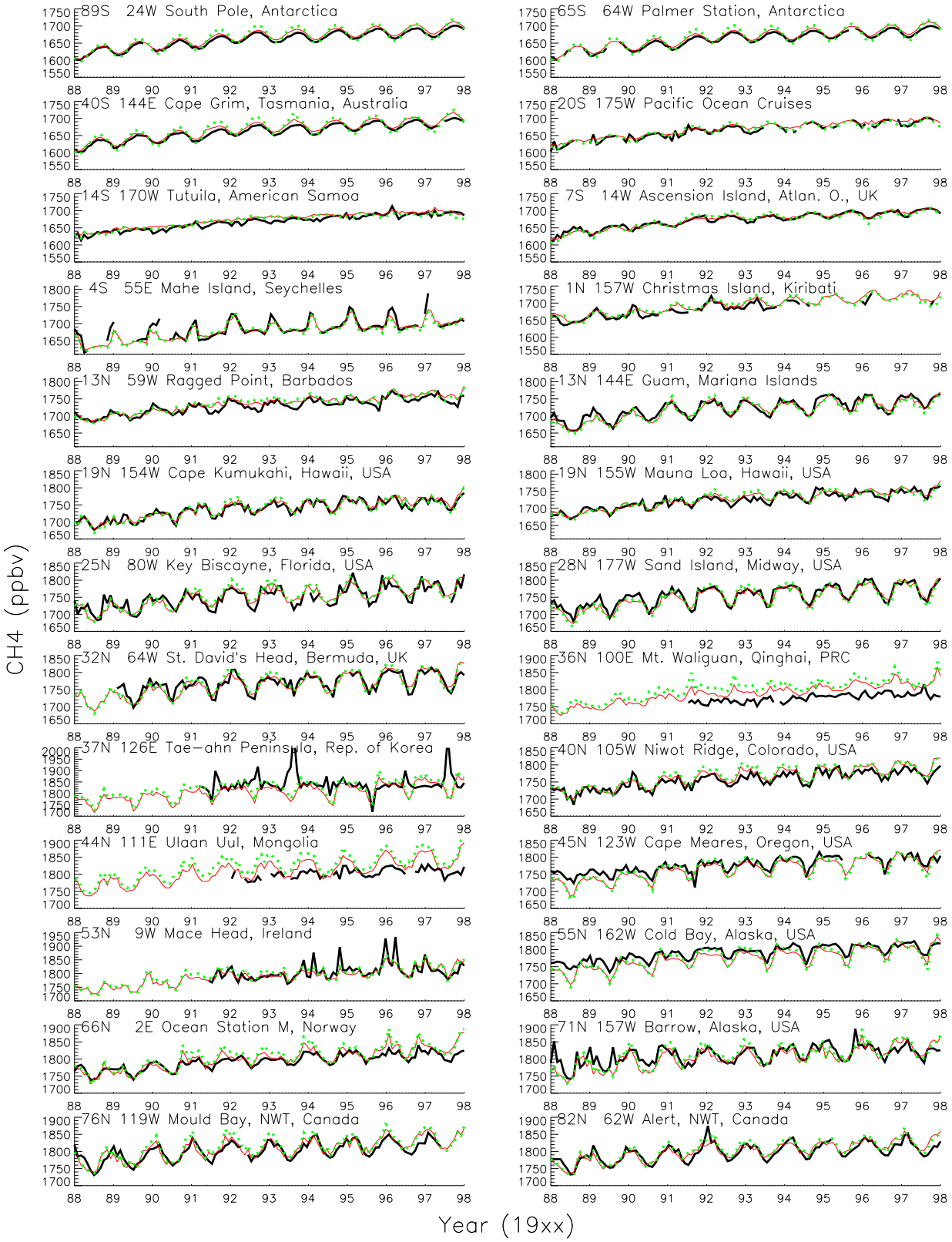

Figure 5. Comparison of results of the "Low OH" (red thin solid lines) and "High OH" (green dotted lines) simulations with observations from a selected subset of CMDL sites (black thick solid lines).

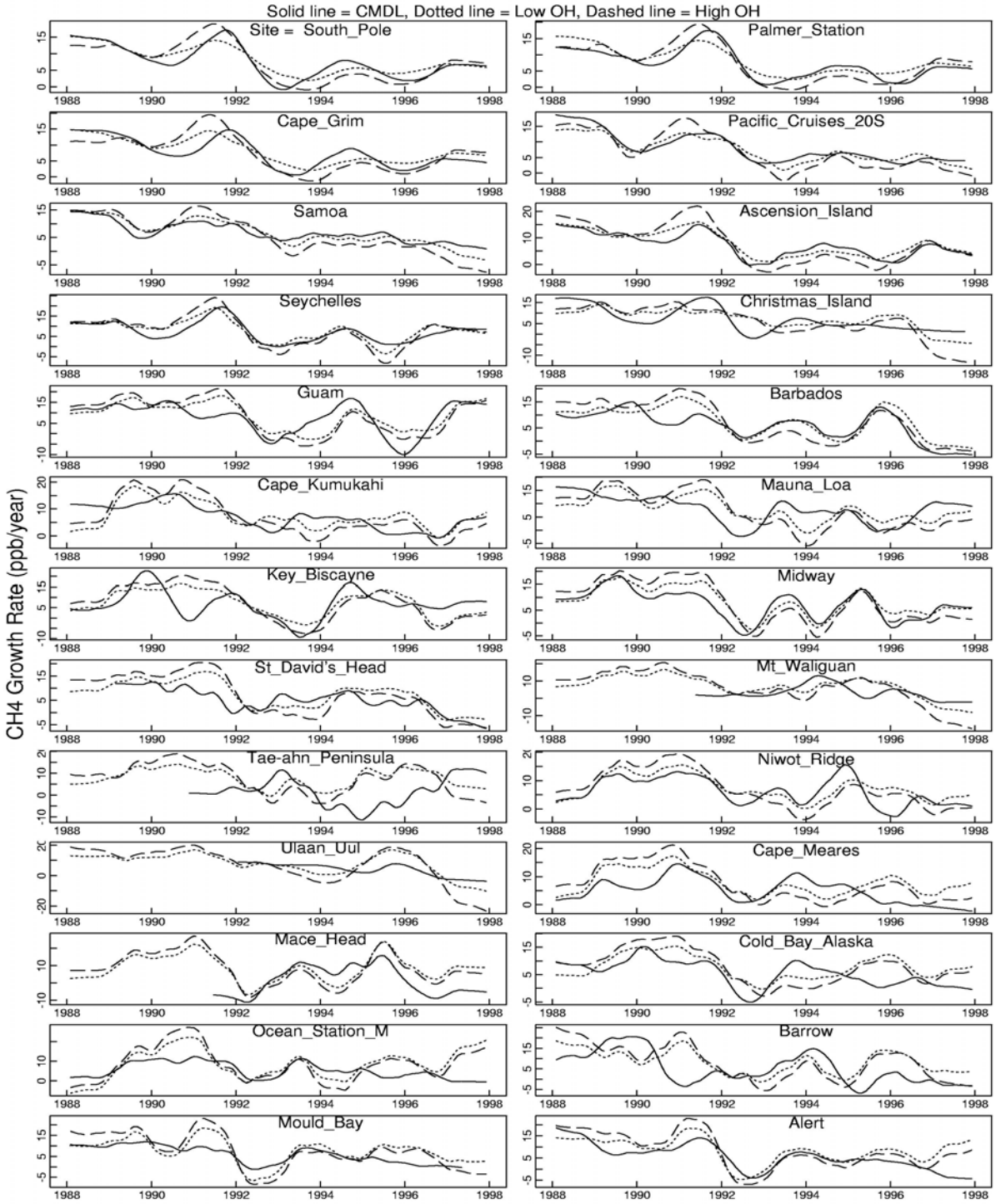

Figure 6. Comparison of instantaneous growth rate time series for model and CMDL observations at selected sites. Included are the "Low OH" and "High OH" simulations.

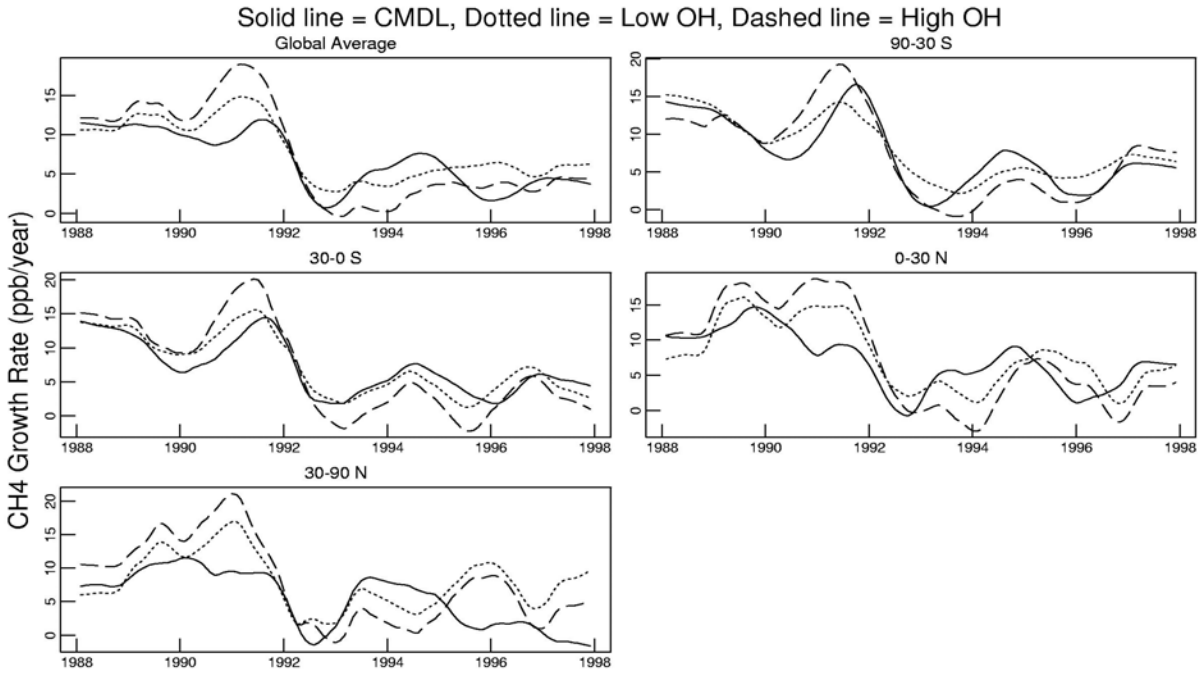

Figure 7. Same as for Figure 6, except the data has been binned into global and semi-hemispheric averages.

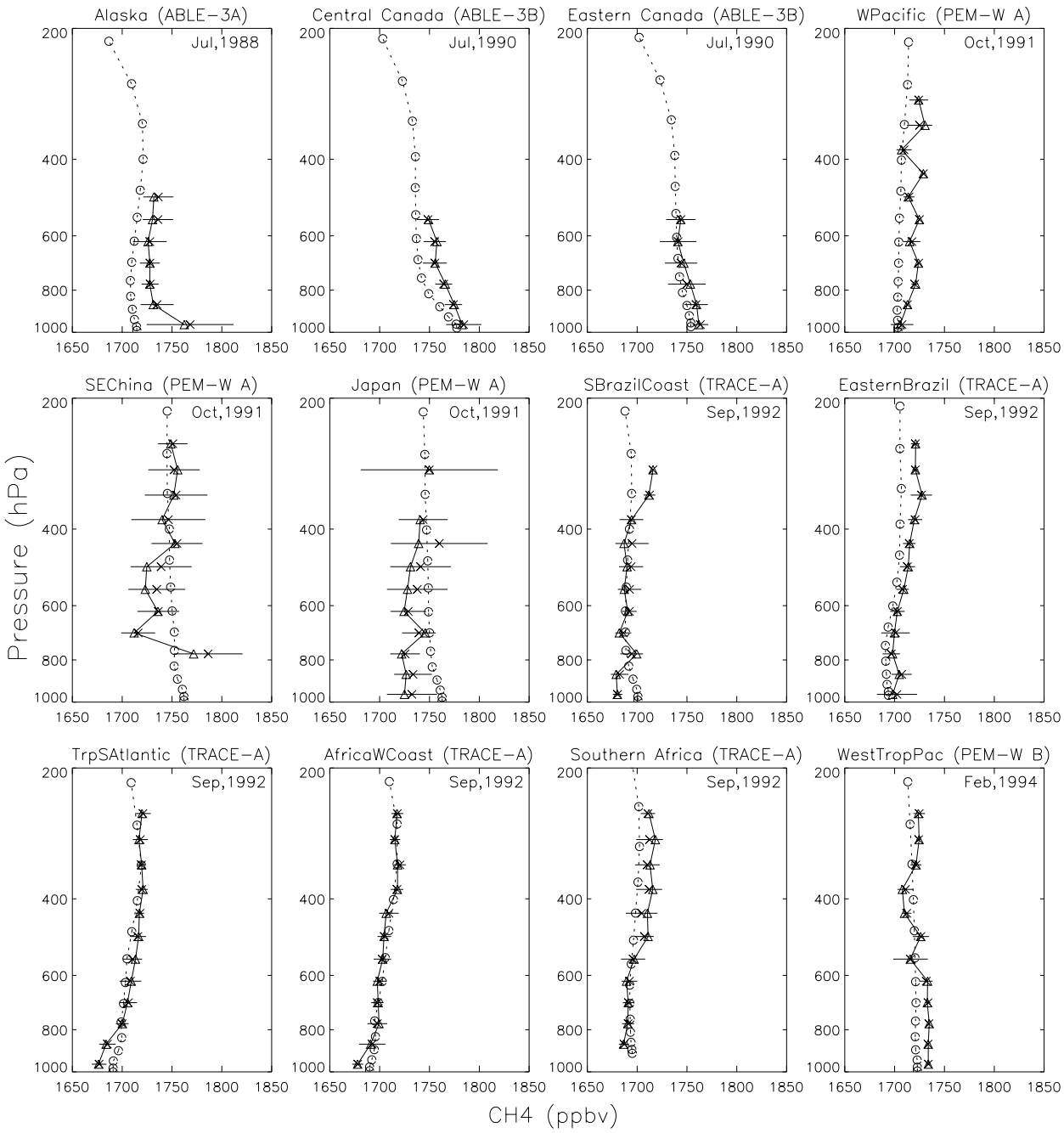

Figure 8. Comparison of model and observed vertical profiles. Results are shown for the "Low OH" simulation (the "High OH" simulation is similar). Triangles connected by solid lines represent observational medians, X's represent observational means, and circles connected by dashed lines represent model results. Horizontal bars indicate standard deviations of the observations. Key to abbreviations: WPacific = Western Pacific, SEChina = Southeastern China, SBrazilCoast = Southern Brazil Coast, TrpSAtlantic = Tropical South Atlantic, WestTropPac = Western Tropical Pacific, MidWPacific = Mid-western Pacific, StPacific = South Tropical Pacific, and (S)EasterIs = (South) Easter Island.

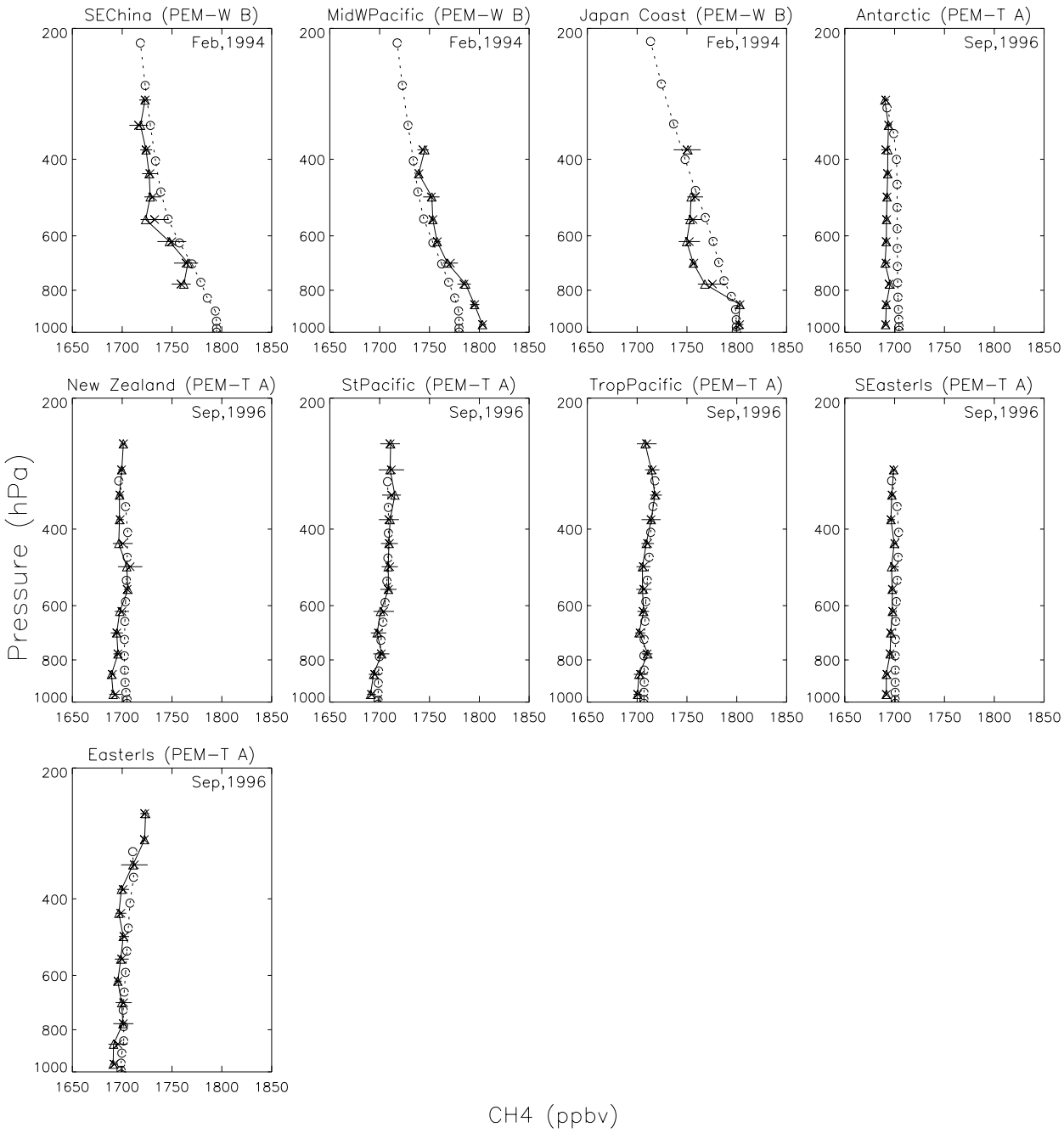

Figure 8. (continued)

a)

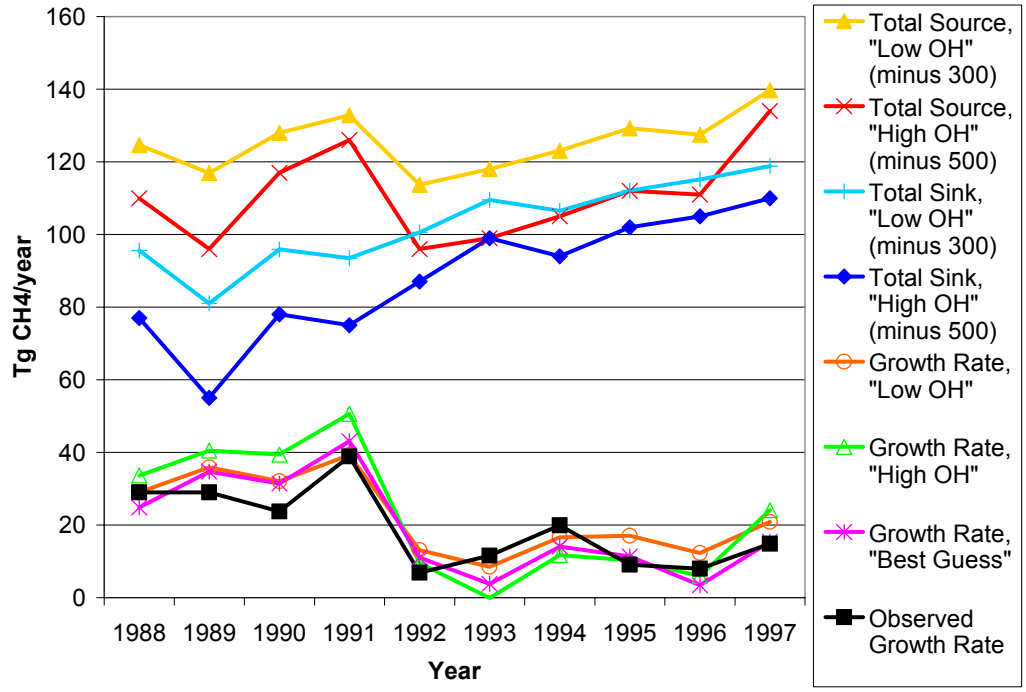

b)

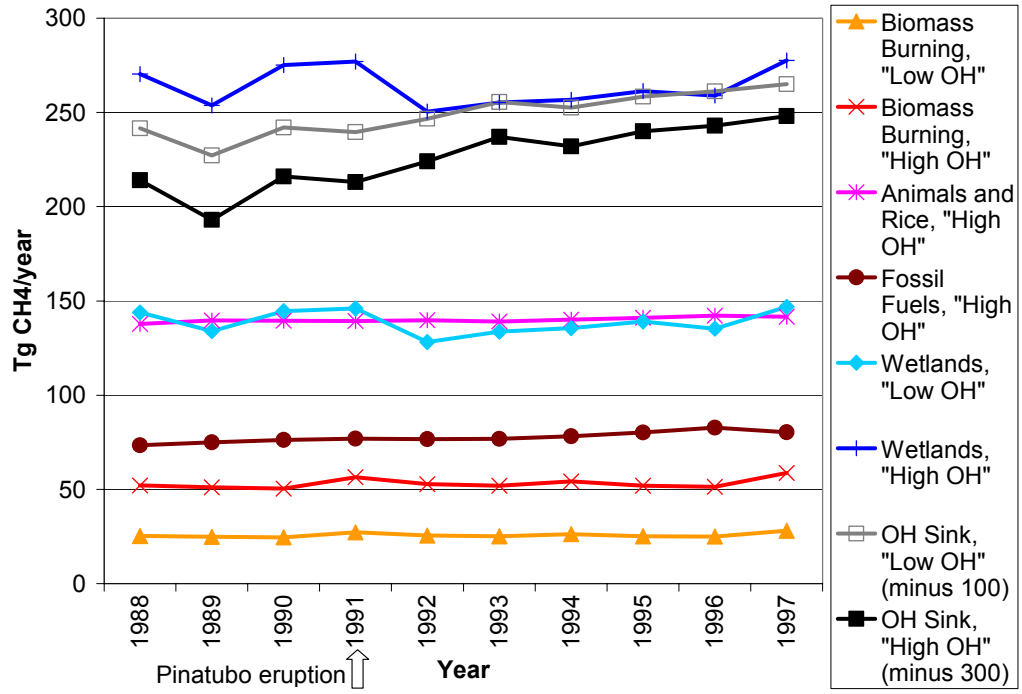

Figure 9. Interannual variations in the methane budget: (a) total source, total sink, and growth rate (net source); (b) individual source and sink types. Observed growth rates in (a) are based on Dlugokencky et al. [2001]. Biomass burning includes biofuel; fossil fuels includes gas leakage, gas venting/flaring, and coal; wetlands includes swamps, bogs, and tundra. "Animals and Rice" and "Fossil Fuels" time series are not shown for the "Low OH" case since they are similar to those for the "High OH" case.

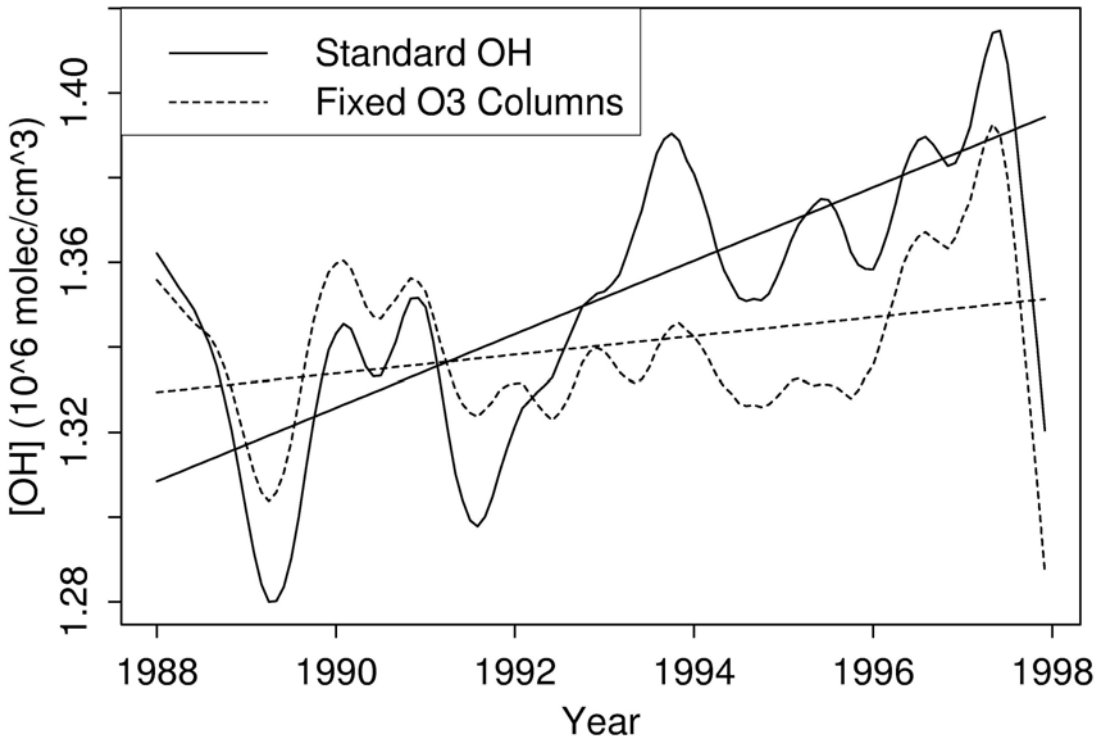

Figure 10. Time series of global average OH. Shown are the standard OH time series based on the work of Duncan et al. [2003b] along with the time series calculated in a sensitivity test in which the O_3 columns were fixed at 1988 levels. The curves are shown deseasonalized and smoothed (loess with span of 1 year) to highlight interannual variations. Included are linear least-squares fits through the two time series. The average trends for the standard and sensitivity runs are +0.64%/year and +0.16%/year, respectively. Note that the concentrations were scaled by a uniform factor of 0.623 in the "Low OH" multi-year CH_4 simulation.